CCEER 88-2

A Micro-CAD System for Seismic Design of Regular Highway Bridges

Donald Orie

Mehdi Saiidi

Bruce Douglas

A Report to

The National Science Foundation

Research Grant ECE-8412576

Civil Engineering Department

University of Nevada, Reno

June 1988

ACKNOWLEDGEMENTS

The study that is presented in this report is part of a continuing investigation at the University of Nevada, Reno (UNR) on the seismic behavior of highway bridges. The project was funded by Grant ECE-8412576 from the National Science Foundation (NSF). The authors are thankful to Dr. S.C. Liu, the Program Manager, for his support. The statements in this report are those of the author and do not necessarily represent the views of NSF.

Special thanks are extended to Dr. Roy Imbsen and his staff of Imbsen and Associates for their helpful comments on the computer modeling segment of the study.

The authors are indebted to the staff of the Nevada Department of Transportation for their valuable comments in the course of this project. Mr. Jim Dodson, the Assistant Director of Operations is thanked for providing helpful information in developing the research proposal. Mr. Rod Johnson, Chief Bridge Engineer, and his staff, Mr. John Terry and Saeed Nafisi, are thanked for reviewing and making many useful suggestions to improve the I/O in Micro-SARB.

ABSTRACT

A microcomputer model for implementing a seismic analysis procedure for bridges is presented. The method is procedure 1 of the Applied Technology Council (ATC-6) document, and is applicable to bridges with "regular" geometry and stiffness along their length.

The input portion of the program was enhanced by interfacing the program with the AutoCAD drafting package. AutoCAD is used to create points and lines which represent nodes and elements.

A parameter study examining the effects of varying the abutment and pier base spring stiffness properties was performed on a five-span reinforced concrete bridge. In addition, the limits of applicability of the computer model are established through a sensitivity study examining the effects of skew angle and curvature in a two-span bridge.

The program was named MicroSARB, and was developed in IBM FORTRAN 77 on an IBM PC-XT. The program can run on an IBM PC, PC-XT, PC-AT, or compatible with a minimum of 256K of memory.

Given the quick turnaround and accessibility of micro-computers, programs like MicroSARB provide a new means by which new and complex design and analysis methods can be transferred to design offices.

TABLE OF CONTENTS

LIST OF TABLES

LIST OF FIGURES

CHAPTER 1

INTRODUCTION

1.1 Introduction

The 1971 San Fernando Valley earthquake was a major turning point toward the development of better seismic design criteria for highway bridges. The damage done to bridges by this earthquake influenced researchers to take a better look at the then current seismic design practices for bridges. Through experimental and analytical studies it was learned that more realistic seismic design methods were needed. In response to this need, the Applied Technology Council (ATC) established new guidelines which incorporated relatively new dynamic analysis techniques. The analysis procedure called for in the ATC guidelines involved a three-dimensional space frame analysis of a bridge. Soon after the guidelines had been developed a mainframe computer program called SEISAB-I was developed, thus providing a means of automating the new guidelines.

Most recently the implementation of microcomputers to solve complex civil engineering problems is becoming more wide spread in design offices. The advent of relatively inexpensive microcomputers which have very good computational capabilities has provided engineers with a more efficient tool for solving problems via old methods. The obvious advantages of using microcomputers for such applications include faster and more accurate results, as

well as an improved presentation of the results. The routine use of microcomputers becomes even more attractive when considering the very low operating costs.

Typically, in the past, computer programs written for most engineering applictions require the user to input or describe the particular problem by generating a data file which contains information about the problem. In addition to solving engineering problems, microcomputers have proven to be quite useful as an advanced drafting tool. In recent years Computer-Aided-Design (CAD) drafting packages have been developed for microcomputers. These widely available CAD drafting systems provide the engineer with an alternate means of describing a particular problem. By interfacing problem solving programs with the CAD programs through linkage codes, which interpret information generated by the CAD program about a particular problem, inputing of the problem can be greatly simplified.

This thesis presents one application of microcomputers in implementing recent seismic design guidelines for highway bridges on the microcomputer. The program being presented uses an analytical procedure described by an Applied Technology Council (ATC) document for seismic design of bridges [2].

1.2 Objective and Scope

The primary objective of this thesis was to develop a microcomputer model which implements procedure 1 of the

ATC-6 document [2] for seismic design of regular highway bridges. In addition, parmeter studies which illustrate various applications of the model, and tests comparing single-modal analysis to multi-modal analysis for regular bridges are presented.

The guidelines for seismic analysis of highway bridges described in the ATC-6 document specify two analysis procedures, one for "regular" bridges and the other for "irregular" bridges. The former utilizes a unimodal approach; where as, the latter considers the multimodal response. A "regular" bridge is described as a bridge with no abrupt changes in mass, stiffness, or geometry along its span. In addition, it may not have large differences in these parameters between adjacent bents. An "irregular" bridge is any bridge not conforming to the definition of a regular bridge.

The ATC guidelines require that bridges be analyzed for seismic forces in two orthogonal directions (longitudinal and transverse directions). The typical procedure for determining seismic forces, even for "regular" bridges, is to perform a space frame analysis of the bridge. To carry out the analysis ATC recommends that any general purpose space frame analysis computer model may be used. In calculating the seismic forces for the unimodal approach the bridge must actually be analyzed twice; once for determining deflections due to a unit load,

and another time for calculating deflections due to seismic forces. This results in many additional intermediate hand calculations. In order to facilitate the application of the ATC-6 guidlines, a special-purpose computer program called SEISAB-I [11], which includes both the unimodal and multimaodal procedures, has been developed.

The computer model is very extensive thus requiring a mainframe computer. Many bridge engineers have limited or no access to mainframe computers, thus making it difficult or impossible to carry out comprehesive space frame analyses. In a recent survey [5], the absence of computer software to implement the ATC-6 guidelines was mentioned as being one of the reasons many practicing engineers are not using the guidelines. It is estimated that more than fifty percent of the highway bridges fall within the "regular" bridge category. Combining this with the notion that microcomputers are genrally available to bridge engineers, it becomes evident that a microcomputer model for implementing the ATC guidelines for regular bridges should be developed. A microcomputer model of this type will encourage bridge engineers to use the new guidelines.

Because of the low operating costs, microcomputer programs of this type will enable designers to vary parameters affecting the behavior of the bridge, thus they are capable of determining even more accurate design forces.

In response to this need, a microcomputer model which performs the ATC-6 analysis for regular highway bridges called "MicroSARB" (Microcomputer Based Seismic Analysis of Regular Highway Bridges) has been developed on an IBM-PC XT using FORTRAN programming language.

The computer model described in this thesis consists of three main segments (1) a preprocessor, (2) an analysis module, and (3) a postprocessor.

1.3 Review of Previous Work Leading to the Development of ATC-6 Procedure 1

The collaspe or partial damage caused to several highway bridges by the 1971 San Fernando Valley earthquake [8,13] stimulated a need for research and development which focused on the seismic analysis and design of bridges. This influenced organizations such as the National Science Foundation and the Federal Highway Administration to sponser analytical and experimental studies which examined various aspects of the seismic behavior of bridges. The extent of the experimental studies ranged from cyclic loading [12] of bridge components to full-scale testing of actual bridges [7]. Many of the analytical studies were aimed at bridges with varying degrees of complexity [3,10,11,17,20]. The findings from these studies, coupled with an increased general knowledge of dynamics of structures, caused researchers and engineers to conclude that substantial revisions were needed in the seismic codes

for highway bridges. In response to this need, the Applied Technology Council established a new set of guidelines for the seismic design of bridges [2]. The guidelines have been adopted by the American Association of State Highway and Transportation Officials (AASHTO) [1] as a "guide" specification and are currently being utilized by many state departments of transportation.

The primary document used for computation of seismic forces in the United States is the standard specifications adopted by AASTHO [1]. Prior to 1973, the standard method of determining seismic forces for bridges involved idealizing each bent as a single degree-of-freedom oscillator with a concentrated static force, representing the earthquake load, applied at the top of the bent. The magnitude of the static load was a fraction of the bridge dead load, ranging between two percent for bridges supported on spread footings to six percent for bridges supported on piles. This method, more commonly known as the "lollipop" method, made certain assumptions that produced inherent error in determining the natural period of the bridge and distribution of the earthquake force to various structural components of the bridge. The assumptions in this method include: (1) each bent vibrates at its own natural frequency, (2) stiffness is provided by the bents only, thus excluding the stiffness of the superstructure. By 1977 the specifications were further

modified to include several factors related to seismicity of the area, bridge dynamic properties, and soil effects. The response spectrum method and dynamic analysis techniques were recommended for relatively complex bridges [10]. An important improvement of the ATC-6 methods over previous seismic design methods is the consideration of the overall behavior of the structure as opposed to the behavior of individual bridge components. SEISAB (SEISmic Analysis of Bridges) is a comprhensive computer program which incorperates this concept in the seismic analysis of bridges. The primary purpose for developing SEISAB was to provide design engineers with a usable tool for implementing the latest seismic design methods. The current program release, SEISAB-I [11], considers both the single-mode and multi-mode response spectrum techniques included in the ATC-6 guidelines. In addition, a second version, SEISAB-II, which includes nonlinear analysis techniques is being developed.

In order to be able to handle a very large range of bridges SEISAB provides for modeling of single column piers as well as multi-column bents, abutments (including walls and bearing pads), expansion joints (including restrainers), pile foundations, and soil properties at the abutments and piers footings. Some of the SEISAB modeling capabilities include the ability to analyze: straight as well as curved bridges, staight or skewed bents, horizontal

or cambered decks, and offset columns or bents.

The central theme behind SEISAB was to provide the design engineer with the most effective means of user-to-program communicaton. SEISAB utilizes a free-formated language input consistent with the natural terminology (ie. bent,pier,column,cap) of bridge engineers. Combining this with its ability to handle such a large variety of bridge configurations, SEISAB is considered as the current state-of-the-art in seismic analysis of bridges.

CHAPTER 2

ANALYTICAL MODELING

2.1 Introduction

In order to account for the directional uncertainty associated with earthquake motions, and the possibility of simultaneous occurance of earthquake forces in two perpendicular directions, the ATC-6 guidelines [2] require that bridges be designed for seismic loads in both the longitudinal and transverse directions. A computer model capable of performing a space frame analysis is required to analyze highway bridges in the transverse direction. For bridges falling in the "irregular" category (nonuniform deck geometry, curved or cambered decks, and skewed or offset bents) the coupling effects between various degrees of freedom (DOF) make a six DOF per node model essential for the analysis of the bridge. When considering the single mode spectral analysis of regular bridges (ATC-6 procedure 1), the uniform geometry of the bridge combined with one directional loading allows for a reduction of the number of DOF's per node needed to model the behavior of the structure if loading in each orthogonal direction is considered seperately.

By creating two separate models, one for loading in the longitudinal direction and the other for loading in the transverse direction, the number of DOF's per node required to model the bridge are reduced to three and four,

respectively. Generally, for most bridges identical bent configurations (and properties) are used throughout the bridge, thus a five-span bridge may have only one or two bent types. With this in mind, the use of substructuring to model the bents becomes inherently favorable. By condensing each bent down to a group of springs representing the overall stiffness of the bent, the bridge superstructure can effectively be modeled as a continuous beam with separate plane frame substructures attached to it.

Hence, by considering each direction separately and utilizing substructuring, a space frame analysis (three-dimensional) is reduced to a series of plane frame (two-dimensional) analyses. Due to somewhat limited memory requirements associated with most personal computers, modeling techniques like those described above become very favorable for implementing structural analysis procedures on microcomputers.

In order to allow for flexibility in modeling various bridge configurations, consideration was given to the types of hinges and bent configurations that are representative of typical highway bridges. Figures 2.1 and 2.2 show hinge and column types which can be modeled on MicroSARB.

The computer model utilizes typical analytical modeling techniques to represent the various components of the bridge. Figure 2.3 illistrates a typical analytical

model using nodes and line elements to represent the bridge superstructure and substructures. Massless line elements are used to model deck, column, and bent cap elements. Structural nodes are assumed to be located at the intersection of piers and deck elements. In addition, one node is assigned to each pier base and each abutment. To account for intermediate hinges additional nodes must be supplied to represent expansion joints and hinges at bents. Because bridge span lengths are relatively large, additional intermediate deck nodes may be included. For columns an additional intermediate node can be included to model non-prismatic columns.

Element stiffness matrices were stored using implicit list processing to minimize memory requirements. The procedure is described in detail in Appendix B.

The ATC-6 procedure 1 calls for the analysis of the bridge twice, once for a uniformly distributed unit load along the length of the bridge and a second time for a non-uniform seismic load along the length of the bridge. (See Fig. 2.4). Additional nodal point loads which represent lumped masses for modeling bent cap weights can be included in the seismic loading. In the model loads are applied through equivalent nodal loads.

2.2 Structural Modeling Techniques - Transverse Direction

This portion of the analytical model was developed to compute the bridge response for horizontal loads in the

transverse direction.

(a) Transverse Degrees of Freedom: Out of the six possible DOF's in a space frame, only four were considered for the deck and upto six were used for the bents for loading in the transvese direction (Fig. 2.5). The deck nodes at bents were allowed to displace in the transverse direction (1 axis) and vertical direction (3 axis), and rotate about the longitudinal direction (2 axis) and vertical direction (3 axis). For intermediate deck nodes the vertical displacement DOF was neglected because very little axial shortening of columns was expected. At deck-to-bent intersections, although axial deformation of individual columns was neglected, the vertical DOF must be included to account for the rotation of the deck due to vertical uplift or settling of pier bases of multi-column bents. For single column piers the vertical displacement will be zero. The deck vertical displacement at the abutment bearings was also restrained because the vertical displacement was expected to have taken place as a result of dead load before lateral loading of the bridge. In bridge structures with monolithic abutments, the assumption is even more valid if no abutment settlement is expected. The longitudinal displacements along the length of the bridge (direction 2) deck are also assumed to be negligible for transverse loading. Generally, the cross-sectional area of a bridge deck is very large making deck axial deformations

very small. For pier bases the vertical DOF was included to account for rotation of multi-column bents; however, rotation about the 3 axis was assumed negligible. This is considered as a reasonable assumption because of the relatively large torsional stiffness of footings, and particularly pile foundations.

(b) Deck Elements: The deck system can be continuous or non-continuous to be able to include the effects of expansion joints. Deck elements were idealized as prismatic line members (Fig. 2.3) which remain elastic in the analysis. Figure 2.6 shows the unrestrained DOF's on a deck element. Because deck length over width ratios can be relatively small, shear deformations for lateral bending were included. Allowing for shear deformations, the stiffness matrix for deck elements becomes

$$[K]_d = \begin{bmatrix} \frac{12R}{L^2} & \frac{6R}{L} & -\frac{12R}{L^2} & \frac{6R}{L} & 0 & 0 \\ & 4R + \gamma R & -\frac{6R}{L} & 2R - \gamma R & 0 & 0 \\ & & \frac{12R}{L^2} & -\frac{6R}{L} & 0 & 0 \\ & & & 4R + \gamma R & 0 & 0 \\ & \text{Symm.} & & & \frac{GJ}{L} & -\frac{GJ}{L} \\ & & & & & \frac{GJ}{L} \end{bmatrix} \quad (2.1)$$

In which

$\gamma = 4\beta$;

$\beta = 3EI/GAL^2$;

A = effective shear area;

E = modulus of elasticity of concrete;

G = shear modulus;

I = moment of inertia about the centroidal axis in the 3 direction;

J = torsional inertia;

L = element length;

$R = EI/[L(1+4\beta)]$.

(c) Column Elements: A column element was assumed to consist of an infinitely rigid top part, and an elastic line element (Fig. 2.7). The infinitely rigid end segment represents the portion of the deck from the centroid of the deck (where a node is located) to the bottom of the deck for monolithic deck-to-column connections (Fig. 2.7). For multi-column bents the rigid end segment may be considered as the distance from the centroid of the bent cap to the bottom of the bent cap. The rigidity of this segment was assumed to be infinity to account for the fact that pier caps (for single column piers) and bent caps (for multi-column bents) are considerably wider than the pier columns. This of course may not always be the case, inwhich case the length of the rigid end block may be assumed zero. For columns, because the axial forces are relativeley small, the axial deformations were neglected.

The deformed shape of a column element, excluding relative displacements of end nodes is shown in Fig. 2.8. The moment-rotation relationship for the elastic region is

$$\begin{Bmatrix} M'_A \\ M_B \end{Bmatrix} = [K'] \begin{Bmatrix} \theta'_A \\ \theta_B \end{Bmatrix} \qquad (2.2)$$

in which

$$[K'] = \frac{1}{\frac{1}{12}\left(\frac{L}{EI}\right)^2 + \frac{SL}{EI}} \times \begin{bmatrix} \frac{L}{3EI} + S & \frac{L}{6EI} - S \\ \text{Symm.} & \frac{L}{3EI} + S \end{bmatrix}$$

where

$S = 1/GAL.$

Refering to Fig. 2.9 the stiffness for the entire element is determined by transforming M'_A to M_A using moment equillibrium of the rigid end segment

$$M_A = (1 + \lambda)M'_A + \lambda M_B$$

The equillibrium equation for the total element can be written as

$$\begin{Bmatrix} M_A \\ M_B \end{Bmatrix} = \underbrace{\begin{bmatrix} 1+\lambda & \lambda \\ 0 & 1 \end{bmatrix}}_{[E]} \begin{Bmatrix} M'_A \\ M_B \end{Bmatrix} \qquad (2.3)$$

The stiffness matrix for the element shown in Fig. 2.8 is determined from

$$[K] = [E][K'][E]^T \qquad (2.4)$$

This matrix does not include the effect of torsion and relative lateral displacements associated with the possible DOF's for column elements (Fig. 2.10). The torsion terms in the stiffness matrix are uncoupled from other terms, thus they can be added independently after the effect of the other deformations have been included. Refering to Fig. 2.11 the relationship between end rotations of the column and lateral displacements is

$$\begin{Bmatrix} \theta_A \\ \theta_B \end{Bmatrix} = [T] \begin{Bmatrix} \delta_A \\ \phi_A \\ \delta_B \\ \phi_B \end{Bmatrix} \qquad (2.5)$$

in which

$$[T] = \begin{bmatrix} \frac{1}{L} & 1 & -\frac{1}{L} & 0 \\ \frac{1}{L} & 0 & -\frac{1}{L} & 1 \end{bmatrix}$$

For the columns of the transversely loaded bridge, bending can take place about both orthogonal directions (axes 1 and

2). (See Fig. 2.5). Including torsional stiffness, the entire column element stiffness matrix becomes

$$[Kp] = \begin{bmatrix} [T]^T[K_L][T] & 0 & 0 \\ 0 & [T]^T[K_V][T] & 0 \\ 0 & 0 & \frac{GJ}{L} \end{bmatrix} \quad (2.6)$$

where $[K_L]$ = stiffness for bending about longitudinal direction (axis 1);

and $[K_V]$ = stiffness for bending about vertical direction (axis 2).

(d) Bent Cap Elements: The bent cap element was assumed to consist of (a) an elastic prismatic middle portion, and at the ends, (b) two infinitely rigid segments (Fig. 2.12). The end segments represent the part of the structure common to both the pier cap and column. The length of the rigid end blocks extends from the centroid of the column to the interior edge of the column. Both axial and shear deformations were assumed to be negligible for the bent cap elements. The permissible DOF's for the bent cap element are shown in Fig. 2.14.

Figure 2.12 shows the deformed shape of a bent cap element excluding relative displacements of end nodes. The relationship between the end moments and end rotations of the flexural portion of the element is as follows

$$\begin{Bmatrix} M'_A \\ M'_B \end{Bmatrix} = \frac{EI}{L} \begin{bmatrix} 4 & 2 \\ 2 & 4 \end{bmatrix} \begin{Bmatrix} \theta'_A \\ \theta'_B \end{Bmatrix} \qquad (2.7)$$

Stiffness Matrix [K']

The stiffness matrix for the entire element, including rigid end segments, is formed by transforming the stiffness matrix in Eq. 2.7. The transformation matrix can be obtained by considering equillibrium of rigid end segments (Fig. 2.13) as

$$M_A = M'_A + A(M'_A + M'_B)$$

or

$$M_A = (1 + A)M'_A + AM'_B$$

in matrix form

$$\begin{Bmatrix} M_A \\ M_B \end{Bmatrix} = \begin{bmatrix} 1 + \lambda_A & \lambda_A \\ \lambda_B & 1 + \lambda_B \end{bmatrix} \begin{Bmatrix} M'_A \\ M'_B \end{Bmatrix} \qquad (2.8)$$

[E]

Finally, the flexural stiffness matrix is determined from

$$[K] = [E][K'][E]^T \qquad (2.9)$$

which is a 2 X 2 matrix consistent with one rotational DOF at each end node.

This matrix is valid for both bending about a longitudinal (axis 2) and vertical (axis 3) direction (Fig. 2.5). However, this matrix must be formulated to include the effects of vertical displacements. This is

accomplished by relating total rotation of the element to rotation due to displacements (Fig. 2.15).

$$\begin{Bmatrix} \theta_A \\ \theta_B \end{Bmatrix} = [T] \begin{Bmatrix} \delta_A \\ \phi_A \\ \delta_B \\ \phi_B \end{Bmatrix} \qquad (2.10)$$

in which

$$[T] = \begin{bmatrix} \frac{1}{L} & 1 & \frac{-1}{L} & 0 \\ \frac{1}{L} & 0 & \frac{-1}{L} & 1 \end{bmatrix}$$

Finally, by considering both bending about the longitudinal and vertical directions (axes 2 and 3), and including the bent cap torsional stiffness, the total bent cap stiffness is expressed in the following form

$$[K]_{\text{bent cap}} = \begin{bmatrix} [T]^T[K_L][T] & 0 & 0 \\ 0 & [T]^T[K_V][T] & 0 \\ 0 & 0 & \frac{GJ}{L} \end{bmatrix}$$

where $[K_L]$ = bent cap rotational stiffness for bending about the longitudinal direction (axis 1);

and $[K_V]$ = bent cap rotational stiffness for bending about the vertical direction (axis 2).

(e) Boundary and Intermediate Hinge Elements: Elastic translational and rotational spring elements were

incorporated to model the effects of abutments, pier bases, and internal deck hinges. All the boundary springs are assumed to be uncoupled. For the abutments one transverse displacement spring and two rotational springs (rotation about directions 2 and 3) are used to model the abutment stiffness including soil effects (Fig. 2.5). Both monolithic and bearing type deck-abutment connections may be modeled. Two translational (directions 1 and 3) springs and one rotational (direction 2) spring are used to model the stiffness properties of footings and pile foundations. Because the abutments and pier base spring elements are located on boundary nodes, the stiffness matrix is simply

$$[K] = \begin{bmatrix} K_1 & 0 & 0 \\ 0 & K_2 & 0 \\ 0 & 0 & K_3 \end{bmatrix}$$

where K_1, K_2, and K_3 are spring stiffnesses of the various translational and rotational springs.

Intermediate deck hinge elements which can be used to model bearing systems for expansion joints, consist of two nodes with two rotational springs and one displacement spring between the nodes (Fig. 2.16). Since this element contains two nodes, the intermediate hinge element stiffness becomes

$$[K]_{hinge} = \begin{bmatrix} K_1 & 0 & 0 & -K_1 & 0 & 0 \\ & K_2 & 0 & 0 & -K_2 & 0 \\ & & K_3 & 0 & 0 & -K_3 \\ & & & K_1 & 0 & 0 \\ & \text{Symm.} & & & K_2 & 0 \\ & & & & & K_3 \end{bmatrix}$$

(f) Substructuring: The use of substructuring at bents required that certain assumptions be made about the degrees of freedom at the bents. The horizontal DOF's associated with the bent cap elements are "slaved" in the transverse direction of the bridge . By modeling the bridge as a series of line elements connected by nodes, the substructure-to-superstructure connection is a single node centrally located at each bent cap. In reality the deck is connected to the bent cap along the entire length of the bent cap. Thus, as the deck translates the bent cap will follow. This is especially true for monolithic connections.

The pier base DOF's are also slaved in the transverse direction, thus it is assumed that the transverse displacement at all pier bases is identical. In multi-column bents, typically each column is supported by individual foundations; however, the footing and pile stiffness are usually the same, and foundation forces are close. The assumption of equal horizontal displacements is

especially true for mat foundations.

In order to account for bending about the vertical direction (axis 3) in multi-column bents, six DOF's are assigned to bent cap and intermediate column nodes (Fig. 2.17). In addition to the four DOF's considered for deck nodes (Fig. 2.5), a translational (direction 2) and a rotational (direction 1) DOF are included. For the node representing the deck and bent node (and the intermediate column nodes of a centrally located column), these two DOF's are omitted.

By accumulating the stiffness contributions of individual bent cap, column, and pier base springs, the bent structural stiffness matrix was constructed. Indices were used to relate local element DOF's to global DOF's. The bent structural matrix was divided so that components related to the four DOF's of the centrally located bent-to-deck connection node were partitioned as described below.

$$\begin{Bmatrix} F_1 \\ F_2 \end{Bmatrix} = \underbrace{\begin{bmatrix} K_{11} & K_{12} \\ K_{21} & K_{22} \end{bmatrix}}_{[K]_{bent}} \begin{Bmatrix} \Delta_1 \\ \Delta_2 \end{Bmatrix} \qquad (2.11)$$

where $\{F_1\}$ = nodal force vector;

$\{F_2\}$ = nodal moment vector = $\{0\}$;

and $[K_{11}]$ is a 4 X 4 matrix.

Then the bent structural matrix was condensed [18] to relate the deck-to-bent forces to displacements and rotations

as $$\{F_1\} = [K]^*\{\Delta_1\} \qquad (2.12)$$

where $$[K]^* = [K_{11}] - [K_{12}][K_{22}]^{-1}[K_{21}]. \qquad (2.13)$$

This matrix in effect represents a group of four springs which are attached to the deck at bent locations.

(g) Overall Bridge Structural Stiffness Matrix: By accumulating contributions of bents, deck elements, intermediate deck hinges, and abutment springs, the overall structural stiffness matrix was constructed. First, element indices relating local to global degrees of freedom were developed. Then, element stiffness matrices were added to the overall structural stiffness matrix at appropriate locations. The bridge structural stiffness matrix was subdivided so that components related to the transverse displacements were placed in the upper left-hand submatrix as follows

$$\begin{Bmatrix} P \\ M \end{Bmatrix} = \begin{bmatrix} K_{11} & K_{12} \\ K_{21} & K_{22} \end{bmatrix} \begin{Bmatrix} U \\ \theta \end{Bmatrix} \qquad (2.14)$$

where $\{P\}$ = equivalent nodal forces;

and $\{M\}$ = equivalent nodal moments.

Then the structural stiffness matrix was condensed to relate known transverse forces to displacemnets as

$$\{P\}^* = [K]^*\{U\} \qquad (2.15)$$

where $$\{P\}^* = \{P\} - [K_{12}][K_{22}]^{-1}\{M\} \qquad (2.16)$$

and $$[K]^* = [K_{11}] - [K_{12}][K_{22}]^{-1}[K_{21}]. \qquad (2.17)$$

2.3 Structural Modeling Techniques - Longitudinal Direction

This part of the analytical model was developed to determine the bridge response for horizontal loads in the longitudinal direction.

(a) Longitudinal Degrees of Freedom: For loading in the longitudinal direction, only three degrees of freedom (DOF's) needed to be considered (Fig. 2.18). All nodes were free to displace in the longitudinal and vertical directions (axes 2 and 3). In addition, all nodes were allowed to rotate about the transverse direction (axis 1).

(b) Deck Elements: Because there is bending about the transverse axis, the deck elements were assumed to consist of an elastic middle portion with infinitely rigid end segments at each end (Fig. 2.12). The length of the rigid end block is the distance from the centroid of the bent cap (where a node is located) to the edge of the transverse diaphragm. At abutments, the distance is taken from the node defined at the end of the deck to the inside edge of the diaphragm.

The unrestrained DOF's on a deck element of the longitudinal model are displayed in Fig. 2.19. Both the axial and vertical shear deformations are neglected. The large axial area of the deck combined with the fact that most of the longitudinal deformation will result from bending of the columns makes these assumptions valid. Figure 2.12 shows the deformed shape of a deck element

excluding relative end displacements. The procedure for determining the longitudinal deck element stiffness matrix is identical to that of the bent cap elements for the transverse model (Sec. 2.2.d). Using Eqs. 2.7 to 2.10 the longitudinal deck element stiffness matrix can be shown to be

$$[K]_{deck} = [T]^T[K_T][T] \qquad (2.18)$$

where $[K_T]$ = deck element rotational stiffness for bending about the transverse direction

and

$$[T] = \begin{bmatrix} \frac{1}{L} & 1 & -\frac{1}{L} & 0 \\ \frac{1}{L} & 0 & -\frac{1}{L} & 1 \end{bmatrix}$$

(c) Column Elements: In the longitudinal direction the column elements are free to rotate about the transverse axis, as well as, translate in the longitudinal direction. The vertical DOF's at both ends of each column are slaved, thus neglecting axial deformations. Identical to the column elements used in the transverse model, the column elements are assumed to consist of an elastic line element with an infinitely rigid end segment at the top of the column (Fig. 2.8). The permissible DOF's for a column element in the longitudinal direction are shown in Fig. 2.20. Including shear deformations and following the

procedure outlined for column elements for the transverse model (Eqs. 2.2 to 2.5), and noting that the torsional DOF is restrained, the stiffness matrix for column elements in the longitudinal direction reduces to

$$[K]_{col} = [T]^T[K][T] \qquad (2.19)$$

where [K] = the column element stiffness matrix for end rotations only;

and [T] = transformation matrix to include relative end displacements.

(d) Bent Cap Elements: The bent cap elements were assumed to be flexible in the torsional sense only (rotation about axis 1, Fig. 2.18). For a line element bridge model it would appear that the bent cap elements are capable of bending about the vertical direction (axis 3). However, for a real bridge the deck is attached to the bent cap along the entire length of the bent cap either continuously (monolithic deck-pier joints) or at several locations (simply-supported decks). Consequently, the deck will prevent rotation of the bent cap about axis 3. In addition, since the deck and bent cap move as a unit, the bent cap ends are not expected to experience any relative displacements. The unrestrained DOF's for longitudinally loaded bent cap elements are displayed in Fig. 2.21. The stiffness matrix for a bent cap element subjected to torsion only is

$$[K]_{\text{bent cap}} = \frac{GJ}{L}\begin{bmatrix} 1 & -1 \\ -1 & 1 \end{bmatrix}$$

where G = shear modulus;

J = torsional inertia;

L = unsupported bent cap length.

(e) Boundary and Intermediate Hinge Elements: Abutment and pier base stiffness properties were idealized using two translational (directions 2 and 3) and one rotational (direction 1) linear elastic springs. In addition, intermediate deck hinge elements comprised of linear elastic translational and rotational springs are used to model expansion joints (Fig. 2.16). The stiffness matrices for single node abutment and pier base springs, and intermediate deck hinges (double node) are identical to those described for the transverse model (Sec. 2.2.e). The only difference being the values of stiffness K_1, K_2, and K_3.

(f) Substructuring: Based on the assumption that the deck and bent caps will not experience rotation about the vertical direction (axis 3), only one longitudinal degree of freedom was assigned to all of the bent cap nodes (Fig. 2.18). The deck and bent cap experience the same displacement in the longitudinal direction. Identical to the transverse model, the longitudinal DOF's at pier bases are "slaved" so that all pier bases displace the same amount. In addition, because axial deformations in column elements

are neglected, all the nodes on an individual column are assigned the same vertical DOF.

Using indices which relate local element DOF's to global DOF's, individual element contributions were accumulated to form the bent structural stiffness matrix. Similar to the transverse bent stiffness matrix, this matrix was divided so that components related to the three DOF's of the central bent-to-deck node were placed in the upper left-hand matrix $[K_{11}]$ (See Eq. 2.11). For the longitudinal bent stiffness matrix, $[K_{11}]$ is a 3 X 3 matrix. Using Eqs. 2.12 to 2.13 the bent stiffness matrix was condensed to represent a group of three springs which attach to the deck at bent locations (Sec 2.2.f).

(h) Overall Bridge Structural Stiffness Matrix: Through element indices relating local to global degrees of freedom, the bridge stiffness matrix was formed. This matrix contains stiffness components from bents, deck elements, abutment springs, and intermediate deck hinges. The bridge stiffness matrix was partitioned (identical to the transverse model) so that components related to the longitudinal displacements were placed in the $[K_{11}]$ matrix of Eq. 2.14. The bridge structural stiffness matrix was condensed so that unknown longitudinal displacements, $\{U\}$ could be calculated using applied equivalent nodal loads, $\{P\}$ and $\{M\}$ (See Eq. 2.15 to 2.17).

CHAPTER 3

SEISMIC LOADS BASED ON ATC-6

3.1 Introduction

Recent advances in dynamics of structures allow design engineers to perform more rigorous dynamic analyses of strucutures. In order to simplify the task of implementing these relatively new and advanced dynamics of structures techniques in the field of bridge engineering, Penzien and Imbsen have developed the Single-Mode Spectral Method (SMSM) [16]. The SMSM is an approximate analytical procedure for obtaining the forces in structural members of highway bridges due to seismic loading. The SMSM can be applied to bridges which can be characterized as having their predominant dynamic response in a single mode of vibration.

Similar to the "lollipop method" , the basis behind the SMSM is that the dynamic forces acting on the bridge result from inertial loading (Fig. 3.1). The primary difference being that the SMSM considers the stiffness of the entire system and not just individual bents.

Procedure 1 of the Applied Technology Council (ATC) document [2] follows the SMSM for analysis of regular highway bridges. A discussion of the ATC-6 clasiffication of bridges, an overview of the SMSM (ATC-6 procedure 1), and a discussion of computer implementation of procedure 1 are presented.

3.2 Applied Technology Council Method (ATC-6)

Included in the ATC-6 document are two procedures for seismic analysis of bridges. Depending on the geometry and location of the bridge, either the SMSM (procedure 1) or a Multi-mode Spectral Method (procedure 2) are specified. The MicroSARB model follows the SMSM, and can be used to analysis regular bridges.

(a) Classification of Bridges: The ATC document [2] includes an acceleration contour map of the United States from which an acceleration coefficient (A) can be determined for various regions of the country. Bridges have been classified into two groups, regular and irregular. A regular bridge is defined as having no abrupt changes in mass, stiffness, or geometry along its length. An irregular bridge is any bridge not defined as regular.

All regular bridges with an acceleration coefficient of 0.09g and higher, as well as, irregular bridges with acceleration coefficients ranging from 0.09g to 0.19g can be analyzed by the unimodal analysis method (procedure 1). An importance classification (IC) is assigned to all bridges located in moderate to severe seismic regions (A > 0.29). The importance factor is an indication of the impact of potential loss associated with a given bridge. Based on the acceleration coefficient and the importance classification, the bridge is assigned to a seismic performance category (SPC) which, in turn, identifies the

analysis procedure to be used.

Consideration to geotechnical characteristics of a given site is included through a site coefficient (S). Response modification factors (R) are used to account for nonlinear action of structural components. These factors tend to reduce internal forces determined from an elastic analysis, and account for redistribution of forces to foundations and abutments.

(b) Single Mode Spectral Analysis Method - Procedure 1: The single mode spectral analysis method outlined in the ATC-6 manual [2] employs Rayleigh's method [4] to determine the single mode response of a bridge. Although bridges are generally continuous systems consisting of many components contributing to the overall stiffness of the system, by assuming a single mode of vibration the bridge can be modeled as a single degree-of-freedom "generalized parameter" model.

Consider the uniformly loaded bridge shown in Fig. 3.2.c. Taking advantage of the fact that free vibration displacements result from inertial forces, it is recognized that the free vibration shape is the deflected shape resulting from loading the bridge with a load proportional to mass of the bridge. Thus, by first applying a uniform unit load P_o so that the bridge deflects into an assumed mode shape $V_s(x)$, and multiplying by a generalized amplitude function, V(t), the dynamic deflection, V(x,t),

of the bridge is generated (See Fig. 3.2).

$$V(x,t) = V_s(x)V(t)$$

The equation of motion for this continuous system approximated by a generalized coordinate is

$$m^*V(t) + c^*V(t) + k^*V(t) = p^*(t) \qquad (3.1)$$

where $m^* = \int m(x)V_s^2(x)dx + \sum m_i V_{si}$

$c^* = \int c(x)[V_s(x)]^2 dx$

$k^* = \int EI(x)[V''(x)]^2 dx$

$= 2 \times$ (max. strain energy due to load P_o)

$$= 2\left[\frac{P_o}{2}\int V_s(x)dx\right]$$

and $p^* = \int p(x,t)V_s(x)dx$.

Note:

$m(x)$ = distributed mass along bridge length;

m_i = additional discrete mass;

V_{si} = corresponding discrete displacements;

$c(x)$ = distributed damping along bridge length;

$EI(x)$ = distributed stiffness along bridge length;

P_o = uniform unit load along bridge length.

For the generalized single-degree-of-freedom system subjected to ground acceleration $V_g(t)$ we have $p(x,t) = -m(x)\ddot{V}_g(t)$, thus

$$p^* = -\ddot{V}_g(t)\int m(x)V_s(x)dx .$$

Noting that $m(x) = w(x)/g$ and dividing Eq. 3.1 by m^* we have

$$\ddot{V}(t) + \frac{c^*}{m^*}\dot{V}(t) + \frac{k^*}{m^*}V(t) = \frac{-\ddot{V}g(t)}{gm^*}\int w(x)V_s(x)dx \qquad (3.2)$$

where

$$\frac{c^*}{m^*} = 2\varepsilon\omega \quad \text{and} \quad \frac{k^*}{m^*} = \omega^2$$

hence

$$2 = \frac{k^*}{m^*} = \frac{gP_o\int V_s(x)dx}{\int w(x)V_s^2(x)dx} .$$

Note that is the undamped natural frequency of the system. If we let

$$\alpha = \int V_s(x)dx \qquad (3.3)$$

$$\beta = \int w(x)V_s(x)dx \qquad (3.4)$$

$$\gamma = \int w(x)V_s^2(x)dx \qquad (3.5)$$

then

$$\omega = \sqrt{\frac{k^*}{m^*}} = \sqrt{\frac{gP_o\alpha}{\gamma}}$$

or

$$T = \frac{2\pi}{\omega} = 2\pi\sqrt{\frac{\gamma}{gP_o\alpha}} \qquad (3.6)$$

and

$$\frac{-\ddot{V}g(t)}{gm^*}\int w(x)V_s(x)dx = \frac{-\ddot{V}g(t)\beta}{g\gamma} .$$

Using the standard acceleration response spectral value C_s in its dimensionless form,

$$C_s = \frac{S_a(\varepsilon,T)}{g} \qquad (3.7)$$

where $S_a(\varepsilon,T)$ is the pseudo acceleration spectral value, or

$$C_s = \frac{1.2AS}{T^{2/3}} \qquad (3.8)$$

where

A = the acceleration coefficient;

S = the site coefficient;

T = the fundamental period;

the maximum response of the system is given by

$$V(x,t)_{max} = V(t)_{max}\, V_s(x)$$

where

$$V(t)_{max} = S_d = \frac{S_a}{\omega^2} = \frac{C_s\, g\, \beta}{\omega^2\, \gamma}$$

thus

$$V(x,t)_{max} = \frac{C_s\, g\, \beta}{\omega^2\, \gamma} V_s(x) \; . \qquad (3.9)$$

An approximate maximum acceleration is given by

$$\omega^2 V(x,t)_{max} \; .$$

Hence, the inertial load which yields the maximum displacement $V(x,t)_{max}$ is given by

$$P_e(x) = m(x)\omega^2 V(x,t)_{max} = \frac{\beta C_s}{\gamma} w(x) V_s(x) \; . \qquad (3.10)$$

This inertial load is then applied to the deck as a non-uniformly distributed load, and the resulting static forces become the psuedo seismic forces.

(c) General Procedure: The step-by-step procedure for

applying the ATC-6 procedure 1 is as follows:

Step 1: Apply a uniform load, P_o, along the length of the bridge. Through a static analysis determine the deflected shape, $V_s(x)$.

Step 2: Calculate parameters α, β, and γ of Eqs. 3.3 to 3.5, respectively.

Step 3: Calculate the fundamental period based on the assumed vibration shape (Eq. 3.6).

Step 4: Determine the seismic coefficient, C_s, and the pseudo inertial load, $P_e(x)$ (Eqs. 3.8 and 3.10) based on an acceleration spectrum.

Step 5: Apply pseudo inertial load, $P_e(x)$, and perform static analysis to determine resulting pseudo seismic displacements and forces.

Step 6: Modify forces based on the response modification factors.

3.3 Implementation

The above procedure was implemented in the MicroSARB model using simple curve fitting and numerical integration techniques. Because the analytical model described in Chapter 2 is a discrete model, a curve must be passed through discrete nodal displacements, and numerical integration of the curve must be performed in order to generate the parameters α, β, and γ (Eqs. 3.3 to 3.5).

(a) Curve Fitting: By applying a uniform unit load, P_o, the bridge is deflected into an assumed mode shape (See Fig.

3.2.c). The true deformed shape is obtained by considering the bridge deck as a continuous system. It should be noted that the bridge may contain discontinuities at hinge locations, but sections of the bridge in between hinges are continuous. In order to perform a static analysis, the bridge is modeled as a discrete system. Thus, only displacements at discrete structural nodes are known (Fig. 3.3.a). Because parameters α, β, and γ (Eqs. 3.3 to 3.5) involve integration of the displaced shape over the entire length of the bridge deck, the intermediate (between nodes) displacements must also be determined.

The displacement function $V_B(x)$ for the bridge is generated by fitting a smooth curve through the known nodal displacements (Fig. 3.3.b). A common curve fitting technique which can be employed to generate a curve is the Least Square's method [25,26]. A problem with this method, and methods of this type, is that for bridge decks modeled with only a few nodes the shape of the curve generated may not effectively represent the true deformed shape. This method becomes even more erroroneous for bridges with intermediate deck hinges. In which case a series of curves are generated. Each curve may contain as few as 2 or 3 nodes.

Another approach to generating the deformed shape of the bridge is the method of cubic splines [23]. The basis behind this method is to fit successive cubic splines

between each superstructure node point. One advantage to this method is that it allows for a closed form solution of the three integrals of Eqs. 3.3 to 3.5. At the same time producing a smooth representation of the displaced shape. The SEISAB-I model employs this method for curve generation [11].

Due to the inaccuracy associated with the Least Square's method, and due to the fact that the method of Cubic Splines requires substantial computer memory, an alternative method of curve generation was used in the MicroSARB model. In MicroSARB, the displacements in between the nodes are determined using the displacements and forces at the boundary nodes for each element.

Once the superstructure nodal displacements, rotations and element end forces (shears and moments) due to a uniform unit load have been determined, a displacement expression for each element can be calculated. Consider an individual deck element subjected to a uniform load w (Fig. 3.4). Cutting the element at a distance x and summing moments at the section (Fig. 3.4.b) leads to

$$M(x) + 1/2wx^2 - V_o x + M_o = 0 . \qquad (3.11)$$

Noting that for a beam in flexure $M(x) = EI(d^2y/dx^2)$, integrating this expression twice, and applying boundary conditions

$$y(x_o) = y_o \quad \text{and} \quad \frac{dy(x_o)}{dx} = \theta_o$$

which are the left-end nodal displacement and rotation determined from the static analysis, the equaiton for the displaced shape is determined. Two constants of integration are generated in the double integration process. These constants are determined based on the above boundary conditions. The summarized expression for the displaced shape is

$$y(x) = \frac{1}{EI}(Ax^4 + Bx^3 + Cx^2 + Dx + E)$$

where

$A = w/24;$

$B = V_o/6;$

$C = -M_o/2;$

$D = [EI\theta_o - wx_o^3/6 - V_ox_o^2/2 + M_ox_o];$

$E = [EI(y_o - \theta_ox_o) + wx_o^4/8 + V_ox_o^3/3 - M_ox_o^2/2].$

Continuity of the displaced shape is assured since equillibrium and compatability are satisfied at each node. (b) Numerical Integration: Evaluation of the fundamental period of vibration, T, and the seismic load, $P_e(x)$, involves the three integrals of Eqs. 3.3 to 3.5. Using the expression for displaces shape, $V_s(x)$, and considering a uniform mass along the length of each deck element, these parameters (α , β , and γ) can be evaluated using a simple numerical integration technique. Consideration was given to both the Trapezoidal rule and Simpson's rule. Both

methods approximate the area under a curve as a summation of trapezoidal areas, thus representing the curve as a series of linear approximations.

Given the simplicity of both methods and the fact that the Simpson's rule is a slight improvement over the Trapezoidal rule, the Simpson's method was chosen. A displacement function, $V_s(x)$, was determined for each deck element. By breaking each deck element into 100 equal increments, numerical integration of Eqs. 3.3 to 3.5 using Simpson's rule becomes very accurate. The example displayed in Fig. 3.5 illistrates the efficiency of the Simpson's rule. In this example the area of a parabola is determined by considering 40 intervals. The error between the exact solution and Simpson's method (0.071%) is insignificant. It is important to keep in mind that the Single Mode Spectral Method is an approximate method, and slight errors in computing the response parameters can be tolerated.

CHAPTER 4

PARAMETRIC STUDIES

4.1 Introduction

Beyond being a tool for implementing the ATC-6 method 1, MicroSARB provides design engineers with an efficient means by which parameter studies may be performed. Because of the low cost running time associated with micro-computers, studies to determine the effects of varying different element stiffness properties can be performed. Through parameter studies the design engineer can obtain a better feel for the behavior of the structure, and thus isolate the more critical elements.

To illustrate one application of the MicroSARB program, a parameter study in which the effects of variations of boundary element stiffnesses on the internal pier forces was done on the Rose Creek Bridge.

In addition, in an attempt to establish reasonable limitations on the degree of skew and curvature that a bridge may have, yet still be analyzed with MicroSARB, a study examing the effects of skew and curvature on the overall seismic design forces (based on a single-mode analysis) is presented.

4.2 Rose Creek Bridge Abutment and Pier Base Study

The methods used by design engineers to determine the stiffness properties of foundations and abutments are

generally approximate and may not always agree with experimental data. The approximations used to calculate stiffness properties can lead to inappropriate design forces in the bridge structure. Through programs like MicroSARB the sensitivity of the bridge response to variations in the stiffness of boundary elements can be determined.

To demonstrate one application of MicroSARB, the Rosecreek Bridge which had been previously subjected to analytical and experimental studies by others [6,7,20], was analyzed to determine the sensitivity of internal pier forces to variations in the stiffnesses of boundary elements. This bridge has uniform mass and stiffness along its length, and hence, can be classified as regular.

a) The Test Bridge: The Rose Creek Bridge located on highway I-80 near Winnemucca, Nevada, is a five-span reinforced concrete multicell box girder bridge with a total length of 400 ft. (Fig. 4.1). The substructure is comprised of four single piers (Fig. 4.2) and pile-supported abutments. The deck is continuous with no intermediate expansion joints. The deck is supported on five elastomeric bearing pads at each abutment.

The superstructure and pier element stiffnesses were calculated based on geometry and concrete properties. The abutment spring stiffnesses were those determined from a previous system identification study of the bridge [21].

The lateral and rotational stiffness of piles were obtained from Ref. 15, in which the stiffnesses were calculated from the pile group geometry and the soil profiles. In order to simplify the evaluation of the results, the stiffness properties of the foundation at bent 2 were used for all bents. Actually the foundations at bents 1 and 4 are slightly "softer."

The critical seismic forces in the Rose Creek bridge are the moment and shear at the base of the piers as well as the forces at the foundations and abutments. The effect of varying boundary element stiffnesses on abutment and foundation forces is direct and significant. However, the effect on pier forces is uncertain. For this reason, only the sensativity of pier moments and shears were examined in this study. Because the pier bases are moment resistant in the transverse direction, but hinged in the longitudinal direction, only transverse loading was considered.

Using MicroSARB the ATC-6 procedure 1 (for "regular" bridges) was applied to the bridge based on an acceleration coefficient of twenty-one percent of gravity (Fig. 4.3). The forces determined did not include the response modification factors specified by ATC because they would only produce a uniform effect. The reference case was taken to be the bridge model with boundary stiffnesses described above.

For the Rose Creek bridge, because the deck ends are

supported on bearing pads, the correlation between stiffness in different directions needed to be taken into account. The value of abutment stiffness for translation in the z direction and the rotational stiffness about the y axis (Fig 4.4) are related because they both depend on the shear stiffness of the indiviual pads. The rotational stiffness about the x axis depends primarily on the normal stiffness of the pads, thus, it can be approximated as an independent variable. The foundation rotational and translational stiffnesses may also be treated as independent parameters. The former is dominated by the pile-soil friction forces, while the latter is controlled by bearing forces between piles and the soil.

b)Discussion of Results: Based on the aforementioned discussions, four independent parameters were varied:

1. Abutment rotational stiffness about the x axis,
2. abutment rotational stiffness about the y axis and the translational stiffness in the z direction,
3. pier foundation rotational stiffness about the x axis, and
4. pier foudation translational stiffness in the z direction.

(i) Effect of Rotational Stiffness at Abutments - It can be observed in Fig. 4.5 that varying the abutment rotational stiffness about the longitudinal axis has little effect on the pier moments and shears. The stiffness in the reference case was taken to be 6×10^6 K-in/rad. The stiffness varies between one-tenth of the reference value

and very large stiffness quantities which approximate fixed (against rotation) abutments. It can be seen that both shears and moments in the piers were insensative to variations in the stiffness. Forces in piers one and four were slightly affected, but the change was only about ten percent.

(ii) Effect of Shear Stiffness at Abutments - The bearing shear stiffness influenced the translational stiffness in the transverse direction (z axis) and rotational stiffness about the vertical direction (y axis) (Fig. 4.4). Therefore, these stiffness values were varied simultaneously. The results are shown in Fig. 4.6. The reference values were 400 K/in for translational stiffness, and 300,000 K-in./rad for the rotational stiffness. The range of stiffnesses used in this study included the value commonly calculated based on bearing pad manufacturers and the stiffness determined through the system identification study. The plots shown in Fig. 4.6 indicate that the shears in piers one and four were the most sensitive parameters. Because these piers are relatively close to the abutments, it is apparent that forces were redistributed to the abutments as the abutment stiffnesses were increased. Forces in the middle piers increased, but at a relatively small rate.

(iii) Effect of Rotational Stiffness at Pier Foundations - Figure 4.7 shows the changes in shears and moments due to

variations of rotational stiffnesses at pier foundations. The stiffness for the reference case was 100,000,000 K-in/rad. It is evident that pier base shears and moments were very sensitive to the variation of rotational stiffness of the pier foudations, particularly when stiffnesses are relatively low. For higher stiffness values (50,000 K-in/rad and higher) the shears and moments remained relatively unchanged. Although the stiffness values are very high, this range of stiffness can not be viewed as infinitely stiff since a significant part of the deck deflection resulted from pier foudation rotation. The curves indicate that for relatively "soft" foundation systems, designers should pay particular attention to obtaining a realistic estimate of the foudations rotational stiffness properties.

(iv) *Effect of Translational Stiffness at Pier Foudations* - The variation of moments and shears as a function of transverse horizontal stiffness (in the z direction) of the pier foundations is shown in Fig. 4.8. The reference stiffness was 5000 K/in. It can be seen that even when doubling or reducing the reference stiffness by a factor of five, the pier forces did not change appreciably. The variation of forces was approximately ten percent.

4.3 The Effects of Skew and Curvature on Regular Bridges

Based on the ATC-6 definition of a "regular" highway bridge, skewed or curved bridges may be classified as

regular, thus the single-mode analysis would apply. This is particularly true for short span bridges where the difference in geometry between adjacent supports would be minimal. MicroSARB is for the analysis of straight bridges with no skew. Since many bridges are with skew or curvature, or both, a sensativity study to determine the degree of skew or curvature which would lead to significant deviations for a straight unskewed model results was performed on a two-span bridge.

The ATC method accounts for the directional uncertainty of earthquake motions by considering a combination of orthogonal forces [2]. The elastic seismic forces resulting from the analyses in the transverse and longitudinal directions must be combined to form two load cases:

Load Case 1 -

Forces = 100% x | Longitudinal | + 30% x | Transverse |

Load Case 2 -

Forces = 100% x | Transverse | + 30% x | Longitudinal |

where

| Transverse | = absolute value of the member stiffness seismic forces resulting from analysis in the transverse direction,

| Longitudinal | = absolute value of the member elastic seismic forces resulting from analysis in the longitudinal direction.

The resulting forces then become the design forces. In

this study the comparison was made using these design forces. The calcualted forces did not include response modification factors since the effects would only be uniform. The study presented was done using SEISAB-I which allows for variation of skew and curvature in the single-mode analysis.

a) Variable Skew Test: In this study the effects of skew on column moments and shears were examined by simultaneously varying the skew (by the same degree) at the abutments and at the bent (Fig. 4.9). The bridge model used for this test was a continuous two-span reinforced concrete bridge with a single two-column bent (Fig 4.10). This bridge is located on Route 113 in California. The total length is 435 ft. The deck and column properties are displayed in Fig. 4.10. In order to simplify the interpretation of final results, the abutments were assumed to be pinned (free to rotate about the y axis) in the transverse direction, and simply-supported in the longitudinal direction (Fig. 4.11). The bent foundation was taken as fixed. The superstructure-to-bent connection is monolithic.

The skew angle was varied as shown in Fig. 4.9. The degree of varying skew ranged from 0 to 25 degrees. Shears, moments, and axial force at the bottom of the left column (See Fig. 4.9) were calculated for loading in the longitudinal and tranaverse directions. The resulting

forces based on a single-mode analysis are displayed in Tables 4.1-4.5. Included in the tables are forces from the direct analysis (Indiv.) and factored forces (Comb.) in accordance with ATC-6 load cases 1 and 2. In addition, the critical moments, shears, and axial force are tabulated. These shears and moments are the largest resultant of the combined transverse and longitudinal results. Although biaxial bending is present, for circular columns, design based on resulant shears and moments is realistic.

The final design forces were tabulated and are displayed in Table 4.6. The reference case is the bridge described in the previous seciton with skew equal to zero degrees.

b) Discussion of Skew Test Results: It can be observed in Tables 4.1 through 4.5 that some individual force components vary significantly with changing skew. However, the more critical design forces; the moment about the z axis due to longitudinal loading (M_Z), the shear in the z direction resulting from longitudinal loading (V_Z), and the axial force induced by transverse loading (P) remain relatively unchanged as a function of varying skew (Fig 4.10).

It can be observed in Table 4.6 that a skew angle between 10 and 15 degrees is the break point at which error becomes significant. For this bridge and bridges with a similar configuration, a skew angle up to 10 to 15 degrees

can be tolerated before the bridge can no longer be analyzed as a straight bridge.

c) Variable Curvature Test: By gradually decreasing the radius of curvature, the effects of curvature on column forces were examined for a two-span bridge (Fig. 4.9). The bridge model used to examine curvature effects is identical to the bridge used in the skew test with the exception of span lengths (Fig. 4.10). For this test a symmetric bridge with equal span lengths of 200 ft. was chosen. This allows for simpler evaluation of the final results.

The radius of curvature varied from infinity (reference case, straight bridge) to 200 ft. (1/R = 0.005). Using SEISAB-I and the ATC-6 single mode analysis method, bottom column forces in the left column (See Fig. 4.9) were calculated. (See Tables 4.7-4.12). Identical to the skew tests, resultant design shears and moments and axial force obtained from combined loads were calculated. These results were tablulated and compared to the reference case (straight bridge, 1/R = 0) (Table 4.13).

d) Discussion of Curvature Test Results: Similar to the skew test, some individual component forces vary significantly with changing curvature (Tables 4.7-4.12). But, the resultant (critical) forces vary only slightly with increasing curvature. Once again, the dominant moment (Mz - Long.), shear (Vx - Long.), and axial force (P - Trans.) do not vary significantly as a function of varying curva-

ture. The results suggest that this bridge may reach a curvature (1/R) as high as 0.0025 (R = 400 ft.) before the straight model analysis can no longer be considered accurate.

4.4 The Effect of Analysis Method

Given the wide range of bridge configurations, it is often difficult to determine if the single-mode spectral approach is sufficient to describe the dynamic behavior of the bridge. In order to examine the validity of the single-mode analysis method as an approximate method for obtaining seismic forces in highway bridges, a study comparing the single-mode analysis and the multi-mode analysis for a two-span bridge was made.

The bridge used in this study is the reference (skew=0) bridge described in section 4.3.a. The results of the multi-mode analysis are presented in Table 4.14.

A Comparison between the single-mode and multi-mode analyses (for the case of zero skew) reveals that the variation of resultant forces between the two analyses is significantly different (Tables 4.1 and 4.14). However, it can be seen that for loading in the transverse direction, the single-mode and multi-mode results are quite close. The percent error between the single-mode and multi-mode results ranged between 0.1 percent for axial force, P and 12 percent for moment, M_z. In the multi-mode analysis for the predominat transverse mode, the period is 0.380 seconds

while the corresponding natural period for the single-mode analysis was 0.383 seconds. The close correlation of period and forces between the two analysis methods indicates tht the fundamental mode of vibration was indeed the predominant mode in the transverse direction.

In the longitudinal direction, the single mode and multi-mode analysis results were very different in some instances. The largest difference was in the M_Z where the single-mode method overestimated the moment magnitude by 25 percent. The lack of close agreement for forces in the longitudinal direction augguests the higher modes of vibration contributed to the response, and the single-mode analysis may not be sufficiently accurate.

The net effect on design forces was either conservative or unconservative depending on the force component. The single-mode method overestimated the resultant moment by 23 percent, and the resultant shear by 13 percent, but it underestimated the axial force by 7 percent.

CHAPTER 5

SUMMARY AND CONCLUSIONS

5.1 Summary

The primary objective of this study was to develop a microcomputer model for implementing procedure 1 of the Applied Technology Council (ATC-6) seismic design guidelines for straight regular highway bridges, and to demonstrate the effectiveness of the model as an analytical tool for performing parameter studies. The model was named MicroSARB, which stands for Microcomputer-Based Seismic Analysis of Regular Highway Bridges.

The ATC-6 procedure 1 employs the Single Mode Spectral Analysis Method (SMSM) for seismic analysis of "regular" highway bridges. The basic assumption behind the Single Mode Spectral Method is that for a bridge with no abrupt change of geometry, mass, and stiffness along its length, the seismic response can be determined by considering only the fundamental mode of vibration of the bridge.

According to ATC-6, regular bridges need to be analyzed twice in each of the transverse and longitudinal directions. One analysis is for a uniform unit load to determine the fundamental mode shape of the bridge, and the other for psuedo seismic loads to determine the design lateral loads. This leads to a space frame analysis in the transverse direction of the bridge.

By developing two separate models (one for each

direction), and incorporating substructuring techniques for bents, the analysis can be simplified. The ATC-6 procedure 1 is a simplified approach, and the bridges which can be analyzed using this method must have a regular geometry. As result, many assumptions which allow for a reduction in the number of degrees of freedom (DOF's) typically required for a three-dimensional analysis of bridges were used to simplify the analysis. These assumptions and the general modeling techniques employed are described in Chapter 2.

An overview of the Single Mode Spectral Analysis Method and a description of the computer implementation of this method are presented in Chapter 3.

Once the microcomputer model was developed, a sensitivity study evaluating the effects of varying abutment and pier base spring forces was performed on the Rose Creek Bridge; a five-span reinforced concrete bridge located in Winnemucca, Nevada. The object of the study was to identify critical boundary elements which would influence the pier forces significantly. This study is described in Chapter 4.

Also included in Chapter 4, is a study establishing limitations on the degree of skew or curvature that a bridge may contain before it can be idealized as a straight bridge and analyzed by MicroSARB.

In order to establish a "rule of thumb" as to the critical degree of skew or curvature which when present

limits the applicability of MicroSARB, two seperate studies evaluating the effects of skew and curvature on internal column forces were done on a two-span bridge.

In addition, in order to evaluate the accuaracy of the MicroSARB model, several tests comparing results from MicroSARB to SEISAB-I for the ATC-6 single mode approach are presented in Appendix A.

5.2 Observations

The sensitivity study presented in Chapter 4 is one application of the microcomputer model. This study revealed that, for the Rose Creek Bridge, the pier base foundation and abutment bearing system flexibility play an important role in determining the lateral design forces of the bridge piers. It can be seen by the results of the study that, for seismic modeling of the bridge, a more accurate determination of the rotational stiffness properties of the pile foundations at the piers is required. The shear stiffness of the elastomeric bearing pads used at abutments was also found to be an important parameter influencing pier forces. It should be noted that the Rose Creek bridge was a single-column system. The above observations may apply to bridges with multi-column piers to a lesser degree.

Based on the results of the skew test presented in Chapter 4, it can be observed that for bridges with a configuration similar to that in the case study, skew

angles of up to 15 degrees can be tolerated before the straight model analysis no longer yields reasonable results. It was also found that bridges with curvatures of up to 0.0025 $ft.^{-1}$ can be treated as regular systems without considerable loss of accuracy.

It is important to keep in mind that the skew and curvature tests considered only one bridge configuration (a two-span, two-column bent bridge). Because each bridge has a unique configuration, for any given bridge the values of acceptable degree of skew and curvature may not necessarily be the same as those obtained in the study presented in Chapter 4.

5.3 Concluding Remarks

Microcomputer programs like MicroSARB can play an important role in transfering advanced analysis and design methods to design offices. Analytical techniques, such as the ATC methods for seismic design of bridges, need to be readily available to designers; otherwise these techiques will not be utilized.

Use of microcomputers to implement complex design and analysis methods leads to more accurate solutions as well as a more efficient means by which to obtain the solutions. Because of the quick turn around and low runtime costs of microcomputers, the designer can readily examine several alternatives and optimize the solution in a relatively short period of time. In the case of MicroSARB, the bridge

engineer can vary different bridge stiffness parameters affecting the seismic behavior of the bridge in an attempt to determine the more critical design parameters.

5.4 Future Considerations

It should be pointed out that MicroSARB is only a first step for implementing the ATC methods on micro-computers. MicroSARB is limited to straight bridge configurations. For the remaining, more complex bridge configurations, a mainframe computer and a program like SEISAB-I are needed to perform a multi-modal analysis. Given the ever increasing speed and memory capacity of microcomputers, implementation of the more involved multi-modal procedure on a microcomputer seems feasible. By using techniques like substructuring and memory efficient storage, a space frame model needed to handle complex bridge geometry configurations, including skewed and curved bridges, can be developed on a microcomputer.

REFERENCES

1. American Association of State Highway and Transportation Officals, "Standard Specification for Highway Bridges," 1977.

2. Applied Technology Council, "Seismic Design Guidelines for Highway Bridges," ATC Report, No. 6, October 1981.

3. Chen, M. and J. Penzien, "Analytical Investigations of Seismic Response of Short, Single, or Multiple Span Highway Bridges," EERC Report 75-4, University of California, Berkeley, January 1975.

4. Clough, Ray W. and Penzien, J., Dynamics of Structures, McGraw-Hill, Inc., New York, N.Y., 1975, pp. 129-137.

5. Dodson, J., "'Seismic Design Guidelines for Highway Bridges' - A Brief Overview Concering Their Use," Proceedings of a Workshop on Seismic Design of Highway Bridges, Reno, Nevada, April 1984.

6. Douglas, B., and W.H. Reid, "Dynamic Tests and System Identification of Bridges," Journal of the Structural Engingeering, ASCE, Vol. 108, No. ST10, October 1982, pp. 2295-2312.

7. Douglas, B., M. Saiidi, J. Richardson, and J. Hart, "Results From High Amplitude Dynamic Tests and Implications for Seismic Design," Proceedings of the Fifeteenth Joint Meeting of U.S. - Japan Panel on Wind and Seismic Effects, UJNR, May 17-20, 1983, 22 pp.

8. Fung, G., R. Lebeau, E. Klein, J. Belevedere, and A. Goldschmidt, "Field Investigations of Bridge Damage in the San Fernando Earthquake," State of California Division of Highways, Preliminary Report, 1971.

9. Gates, J.H. and M.J. Smith, "Verification of Dynamic Modeling Methods by Prototype Excitation," California Department of Transportation, Report No. FHWA/CA/SD-82/07, Sacramento, Calif., November 1982.

10. Gillies, A. G. and R. Shepherd, "Dynamic Inelastic Analysis of a Bridge Structure," Bulletin of Seismological Society of America, Vol. 72, No. 2, March 1981, pp. 517-530.

11. Imbsen, R., J. Lea, V. Kaliakin, K. Perano, J. Gates, and S. Perano, "SEISAB-I - Seismic Analysis of Bridges

a User Manual," Engineering Computer Corporation Report, October 1982, 94 pp.

12. Imbsen, R.A. and R. Schamber, "Earthquake Resistant Bridge Bearings," Report No. FHWA/RD-82/165, May 1982.

13. Jennings, P.C. and J.H. Wood, "Earthquake Damage to Freeway Structures," Engineering Features of the San Fernando Earthquake, Paul Jennings, Editor, 1973, pp. 279-366.

14. McCalla, Thomas R., Introduction to Numerical Methods and FORTRAN Programming, 1967, pp. 239-250.

15. Norris, G., "Evaluation of the Nonlinear Stablized Rotational Stiffness of Pile Groups," Proceedings of the Third ASCE/EMO Conference on Dynamics of Structures, Los Angeles, California, April 1986.

16. Penzien, J. and Imbsen R., "Seismic Analysis of Bridges a Single Mode Spectral Approach," Proceedings Advances in Earthquake Engineering, University of California, Berkeley, June, 1980.

17. Penzien, J., R. Imbsen, and W. Liu, "NEABS - Nonlinier Earthquake Analysis of Bridge Systems," EERC Report, University of California, Berkeley, May 1981.

18. Przemieniecki , J., Theory of Matrix Structural Analysis, New York, McGraw-Hill, 1968, pp. 147-148.

19. Saiidi, M. and B. Douglas, "Effects of Design Seismic Loads on a Highway Bridge," Journal of Structural Engineering, Vol. 110, No. 11, November, 1984, pp. 2723-2737.

20. Saiidi, M. and J.D. Hart, "Nonlinear Seismic Response of Short Reinforced Concrete Highway Bridges," Proceedings of the Eighth World Conference on Earthquake Engineering, San Francisco, July 1984, Vol. V, pp. 191-199.

21. Saiidi, M., J. Hart, and B. Douglas, "Inelastic Static and Dynamic Analysis of Short R/C Bridges Subjected to Lateral Loads," Civil Engineering Department, Report No. CCEER-84-03, University of Nevada, Reno, July 1984, 99 pp.

22. Saiidi, M. and M. Sozen, "Simple and Complex Models for Nonlinear Concrete Structures, Series 465, Civil Engineering Studies, University of Illinois, Urbana-

Champaign, August 1979, pp. 16-19.

23. Shoup, Terry E., Numerical Methods for the Personal Computer, Prentice-Hall Inc., Englewood Cliffs, NJ, 1983.

24. "The AutoCAD™ Drafting Package," User Guide, Autodesk Inc., April 9, 1985, 339 pp.

25. Wang, P., Numerical and Matrix Methods in Structural Mechanics, With Aplications to Computers, New York, Wiley, 1966 pp. 176-178.

26. Wolfe and Koelling, Basic Engineering and Scientific Programs for the IBM PC

Table 4.1 - Skew Test - Bottom Column - Skew = 0 deg.

Test the Effect of Skew

Two Span Bridge - Two Column Bent Skew = 0 deg.

(Bottom Column) Units = KIP and FT

		Mx	Mz	Vx	Vz	P
(Indiv.)	Trans.	20390.0	495.1	38.1	1465.0	1675.0
	Long.	18.6	32170.0	2212.0	2.1	15.6
(Comb.)	Trans.	20395.6	10146.1	701.7	1465.6	1679.7
	Long.	6135.6	32318.5	2223.4	441.6	518.1

Resultant (Critical) M = 32896

Resultant (Critical) V = 2267

Critical P = 1680

Table 4.2 - Skew Test - Bottom Column - Skew = 0 deg.

Test the Effect of Skew

Two Span Bridge - Two Column Bent Skew = 5 deg.

(Bottom Column) Units = KIP and FT

		Mx	Mz	Vx	Vz	P
(Indiv.)	Trans.	20310.0	2343.0	165.9	1459.0	1666.0
	Long.	2758.0	32050.0	2204.0	197.8	156.7
(Comb.)	Trans.	21137.4	11958.0	827.1	1518.3	1713.0
	Long.	8851.0	32752.9	2253.8	635.5	656.5

Resultant (Critical) M = 33928

Resultant (Critical) V = 2342

Critical P = 1713

Table 4.3 - Skew Test - Bottom Column - Skew = 10 deg.

Test the Effect of Skew

Two Span Bridge - Two Column Bent Skew = 10 deg.

(Bottom Column) Units = KIP and FT

		Mx	Mz	Vx	Vz	P
(Indiv.)	Trans.	20070.0	3177.0	215.6	1442.0	1646.0
	Long.	5440.0	31700.0	2178.0	387.6	262.9
(Comb.)	Trans.	21702.0	12687.0	869.0	1558.3	1724.9
	Long.	11461.0	32653.1	2242.7	820.2	756.7

Resultant (Critical) M = 34606

Resultant (Critical) V = 2388

Critical P = 1725

Table 4.4 - Skew Test - Bottom Column - Skew = 15 deg.

Test the Effect of Skew

Two Span Bridge - Two Column Bent Skew = 15 deg.

(Bottom Column) Units = KIP and FT

		Mx	Mz	Vx	Vz	P
(Indiv.)	Trans.	19680.0	4973.0	339.3	1414.0	1610.0
	Long.	8121.0	31120.0	2134.0	578.5	392.6
(Comb.)	Trans.	22116.3	14309.0	979.5	1587.6	1727.8
	Long.	14025.0	32611.9	2235.8	1002.7	875.6

Resultant (Critical) M = 35500

Resultant (Critical) V = 2450

Critical P = 1728

Table 4.5 - Skew Test - Bottom Column - Skew = 25 deg.

Test the Effect of Skew

Two Span Bridge - Two Column Bent Skew = 25 deg.

(Bottom Column) Units = KIP and FT

		Mx	Mz	Vx	Vz	P
(Indiv.)	Trans.	18450.0	8425.0	575.1	1324.0	1498.0
	Long.	13290.0	29280.0	1997.0	944.3	615.5
(Comb.)	Trans.	22437.0	17209.0	1174.2	1607.3	1682.7
	Long.	18825.0	31807.5	2169.5	1341.5	1064.9

Resultant (Critical) M = 36961

Resultant (Critical) V = 2551

Critical P = 1683

Table 4.6 - Comparison for Variable Skew Test

Test the Effect of Skew

Two Span Bridge - Two Column Bent

(Bottom Column) **Units = KIP and FT**

Design Forces

Skew (degrees)	Moment	% Error	Shear	% Error	Axial	% Error
0	32896	-	2267	-	1680	-
5	33928	3.0	2342	3.2	1713	1.9
10	34606	4.9	2388	5.1	1725	2.6
15	35500	7.3	2450	7.5	1728	2.8
25	36961	11.0	2551	11.1	1683	0.2

Table 4.7 - Curvature Test - Bottom Column - 1/R = 0

Test the Effect of Curvature

Two Span Bridge - Two Column Bent 1/R = 0

(Bottom Column) Units = KIP and FT

		Mx	Mz	Vx	Vz	P
(Indiv.)	Trans.	18060.0	0.0	0.0	1298.0	1488.0
	Long.	0.0	30390.0	2106.0	0.0	0.0
(Comb.)	Trans.	18060.0	9117.0	631.8	1298.0	1488.0
	Long.	5418.0	30390.0	2106.0	389.4	446.4

Resultant (Critical) M = 30869

Resultant (Critical) V = 2142

Critical P = 1488

Table 4.8 - Curvature Test - Bottom Column - 1/R = 0.0005

Test the Effect of Curvature

Two Span Bridge - Two Column Bent 1/R = 0.0005

(Bottom Column) Units = KIP and FT

		Mx	Mz	Vx	Vz	P
(Indiv.)	Trans.	18070.0	13.7	1.2	1299.0	1488.0
	Long.	780.1	30510.0	2114.0	55.6	32.3
(Comb.)	Trans.	18304.0	9166.7	635.4	1315.7	1497.7
	Long.	6201.1	30514.1	2114.4	445.3	478.7

Resultant (Critical) M = 31138

Resultant (Critical) V = 2161

Critical P = 1498

Table 4.9 - Curvature Test - Bottom Column - 1/R = 0.001

Test the Effect of Curvature

Two Span Bridge - Two Column Bent 1/R = 0.001

(Bottom Column) Units = KIP and FT

		Mx	Mz	Vx	Vz	P
(Indiv.)	Trans.	18110.0	20.2	1.8	1301.0	1492.0
	Long.	1557.0	30590.0	2120.0	111.0	64.4
(Comb.)	Trans.	18577.1	9197.2	637.8	1334.3	1511.3
	Long.	6990.0	30596.1	2120.5	501.3	512.0

Resultant (Critical) M = 31384

Resultant (Critical) V = 2179

Critical P = 1511

Table 4.10 - Curvature Test - Bottom Column - 1/R = 0.00125

Test the Effect of Curvature

Two Span Bridge - Two Column Bent 1/R = 0.00125

(Bottom Column) Units = KIP and FT

		Mx	Mz	Vx	Vz	P
(Indiv.)	Trans.	18140.0	20.7	1.9	1303.0	1494.0
	Long.	1944.0	30620.0	2122.0	138.6	80.5
(Comb.)	Trans.	18723.2	9206.7	638.5	1344.6	1518.2
	Long.	7386.0	30626.2	2122.6	529.5	528.7

Resultant (Critical) M = 31504

Resultant (Critical) V = 2188

Critical P = 1518

Table 4.11 - Curvature Test - Bottom Column - 1/R = 0.0025

Test the Effect of Curvature

Two Span Bridge - Two Column Bent 1/R = 0.0025

(Bottom Column) Units = KIP and FT

		Mx	Mz	Vx	Vz	P
(Indiv.)	Trans.	18380.0	38.3	2.8	1321.0	1515.0
	Long.	3848.0	30680.0	2124.0	274.3	162.1
(Comb.)	Trans.	19534.4	9242.3	640.0	1403.3	1563.6
	Long.	9362.0	30691.5	2124.8	670.6	616.6

Resultant (Critical) M = 32088

Resultant (Critical) V = 2228

Critical P = 1564

Table 4.12 - Curvature Test - Bottom Column - 1/R = 0.005

Test the Effect of Curvature

Two Span Bridge - Two Column Bent 1/R = 0.005

(Bottom Column) Units = KIP and FT

		Mx	Mz	Vx	Vz	P
(Indiv.)	Trans.	19340.0	186.6	13.8	1390.0	1599.0
	Long.	7354.0	30280.0	2087.0	524.3	324.2
(Comb.)	Trans.	21546.2	9270.6	639.9	1547.3	1696.3
	Long.	13156.0	30336.0	2091.1	941.3	803.9

Resultant (Critical) M = 33066

Resultant (Critical) V = 2293

Critical P = 1696

Table 4.13 - Comparison for Variable Curvature Test

Test the Effect of Curvature

Two Span Bridge - Two Column Bent R = Radius of Curve

(Bottom Column) Units = KIP and FT

	Design Forces					
1/R	Moment	% Error	Shear	% Error	Axial	% Error
0	30869	-	2142	-	1488	-
.00050	31138	0.9	2161	0.9	1498	0.7
.00100	31384	1.6	2179	1.7	1511	1.5
.00125	31504	2.0	2188	2.1	1518	2.0
.00250	32088	3.8	2228	3.9	1564	4.9
.00500	33066	6.6	2293	6.6	1696	12.3

Table 4.14 - Multi-mode Analysis for Zero Skew Bridge

Multi-mode Analysis for Zero Skew Bridge

Two Span Bridge - Two Column Bent Skew = 0 deg.

(Bottom Column) Units = KIP and FT

		Mx	Mz	Vx	Vz	P
(Indiv.)	Trans.	20510.0	562.9	43.5	1480.0	1673.0
	Long.	550.9	25690.0	1921.0	63.6	462.2
(Comb.)	Trans.	20675.3	8269.9	619.8	1499.1	1811.7
	Long.	6703.9	25858.9	1934.0	507.6	964.1

Resultant (Critical) M = 26714

Resultant (Critical) V = 2000

Critical P = 1812

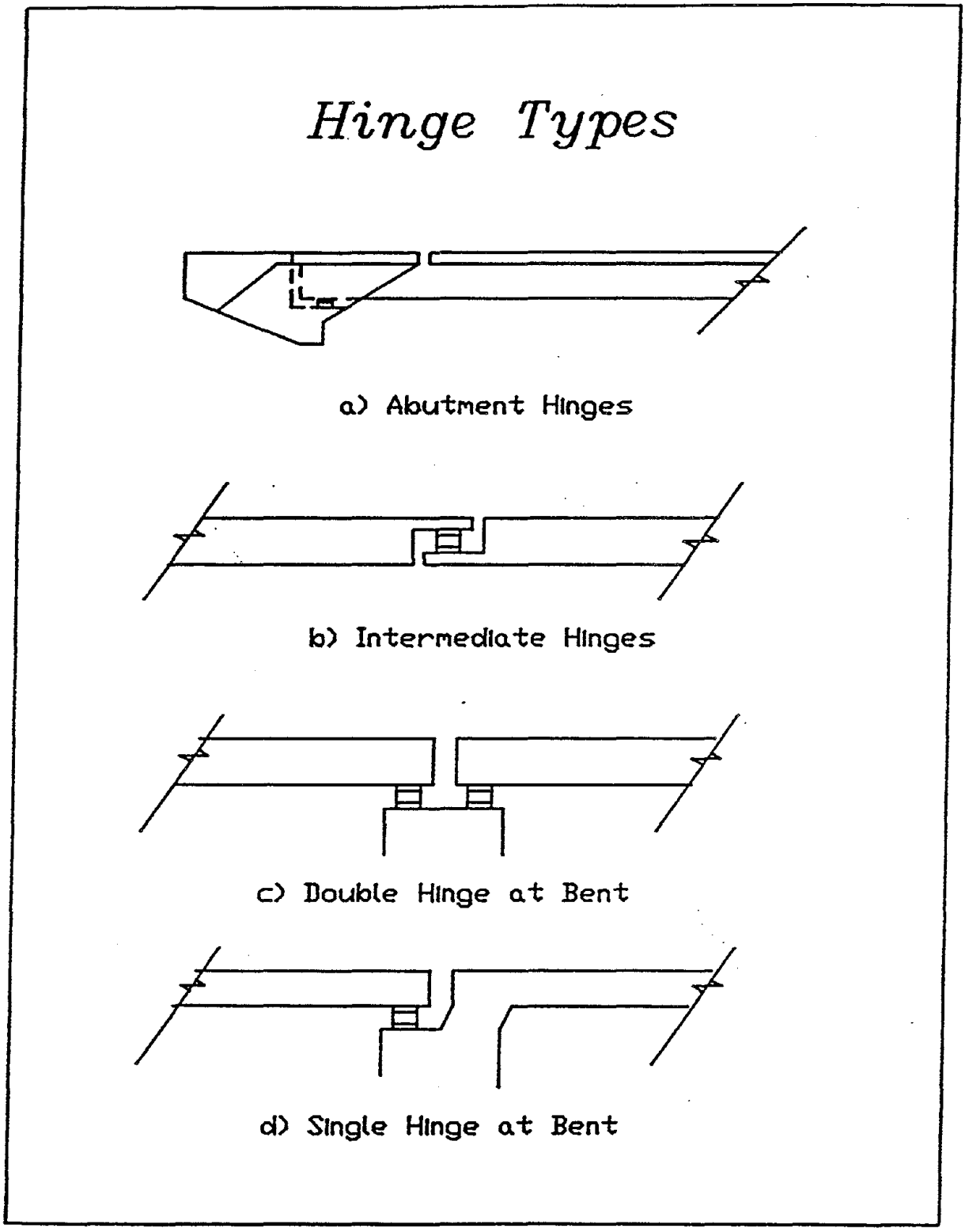

Figure 2.1 - Intermediate Deck Hinges

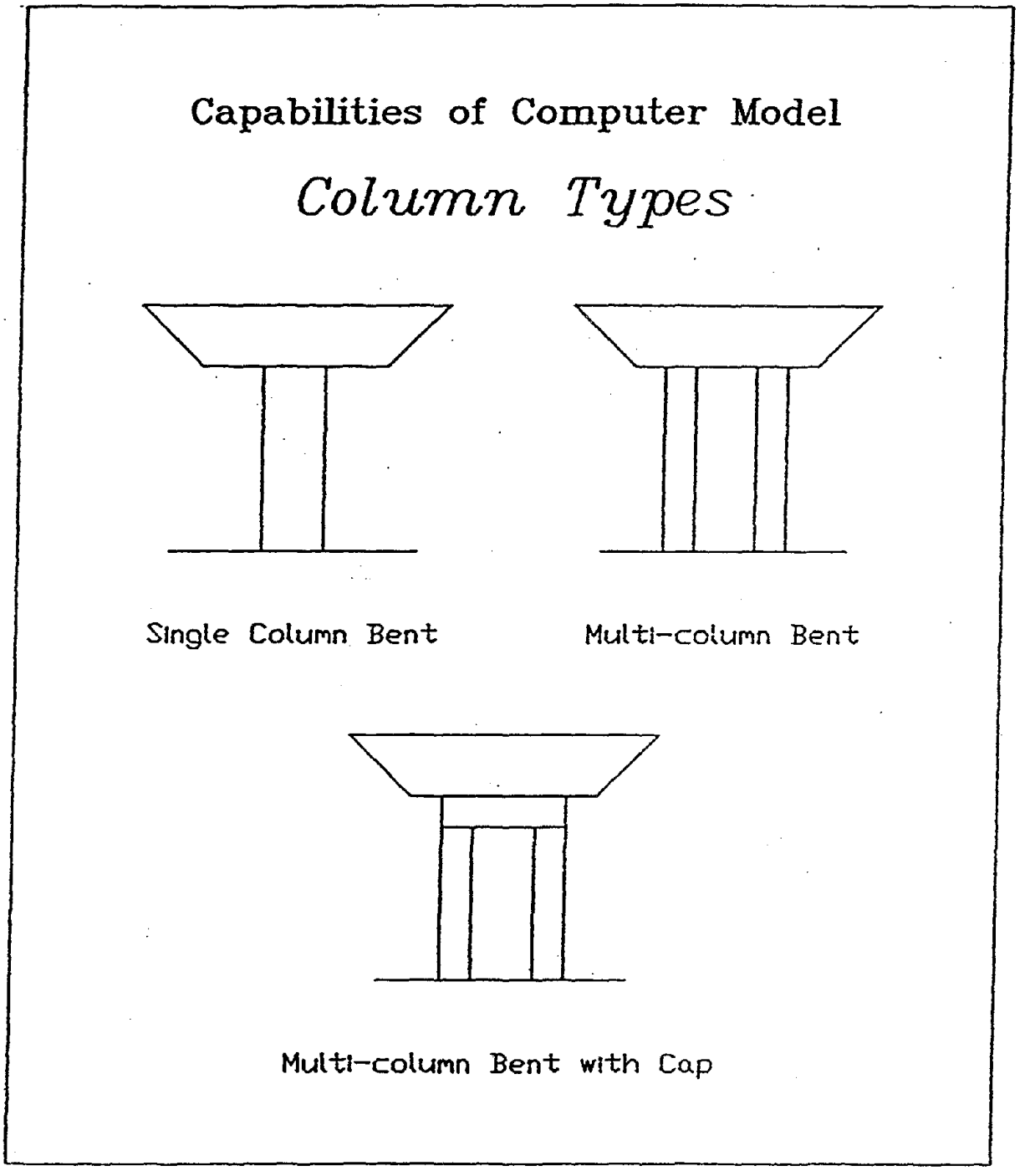

Figure 2.2 - Columns Types

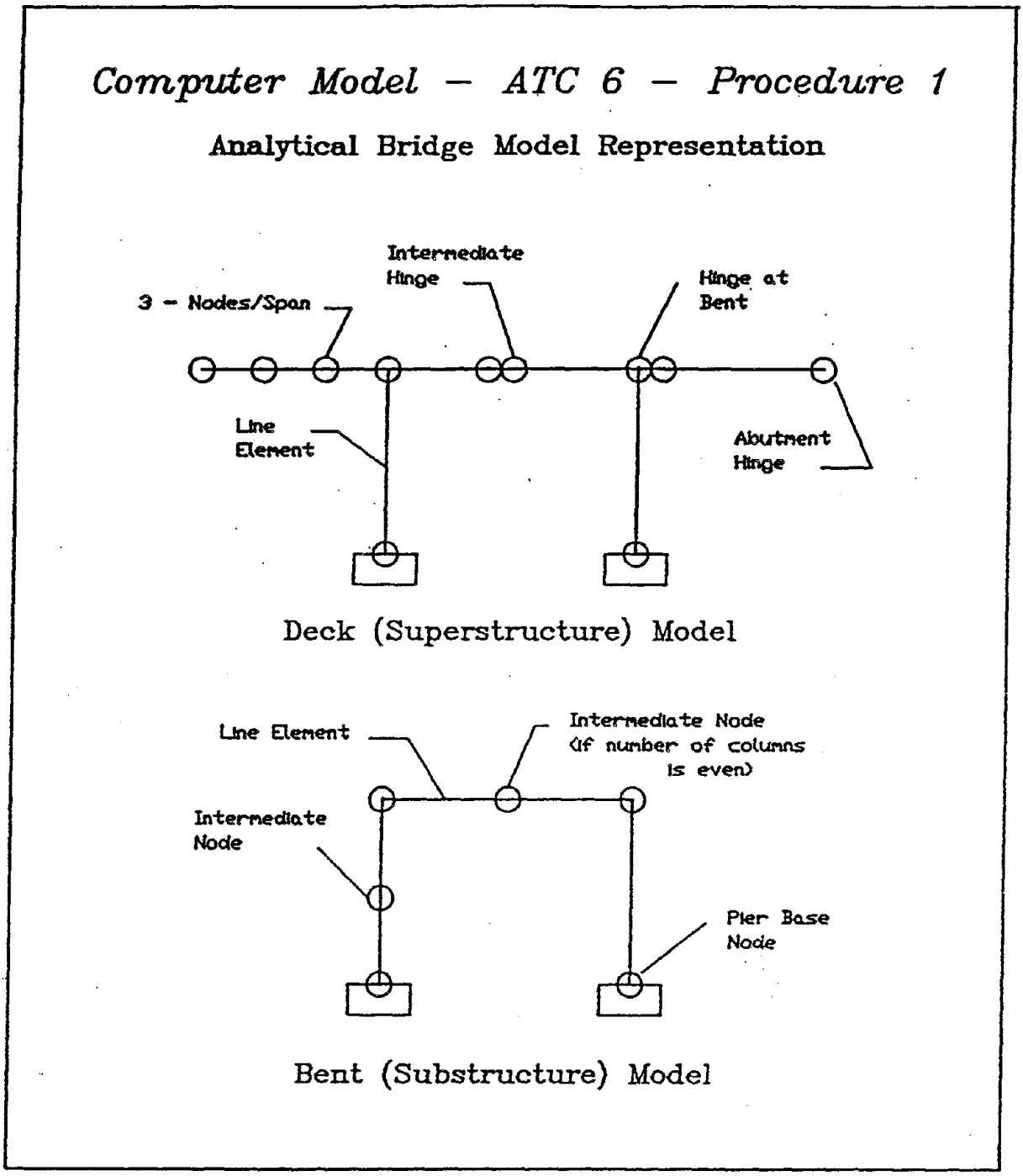

Figure 2.3 - Analytical Bridge Model Presentation

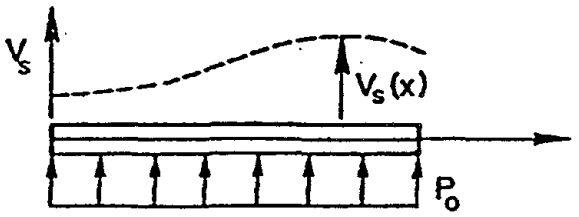

(a) Plan-Transverse Unit Loading

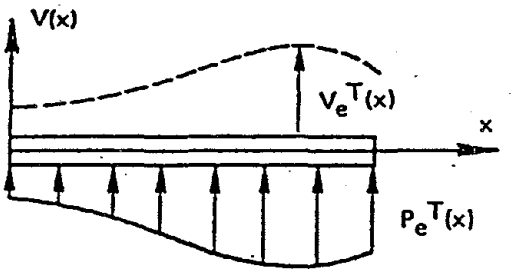

(b) Plan-Transverse Seismic Loading

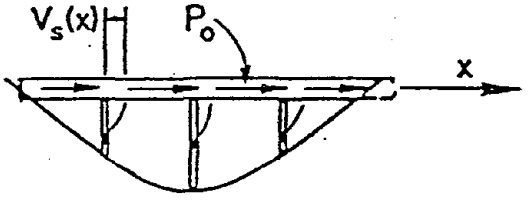

(c) Elevation-Longitudinal Unit Loading

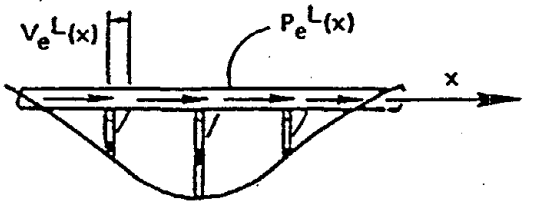

(d) Elevation-Longitudinal Seismic Loading

Figure 2.4 - ATC-6 Procedure 1 - Uniform Unit and Seismic Loading

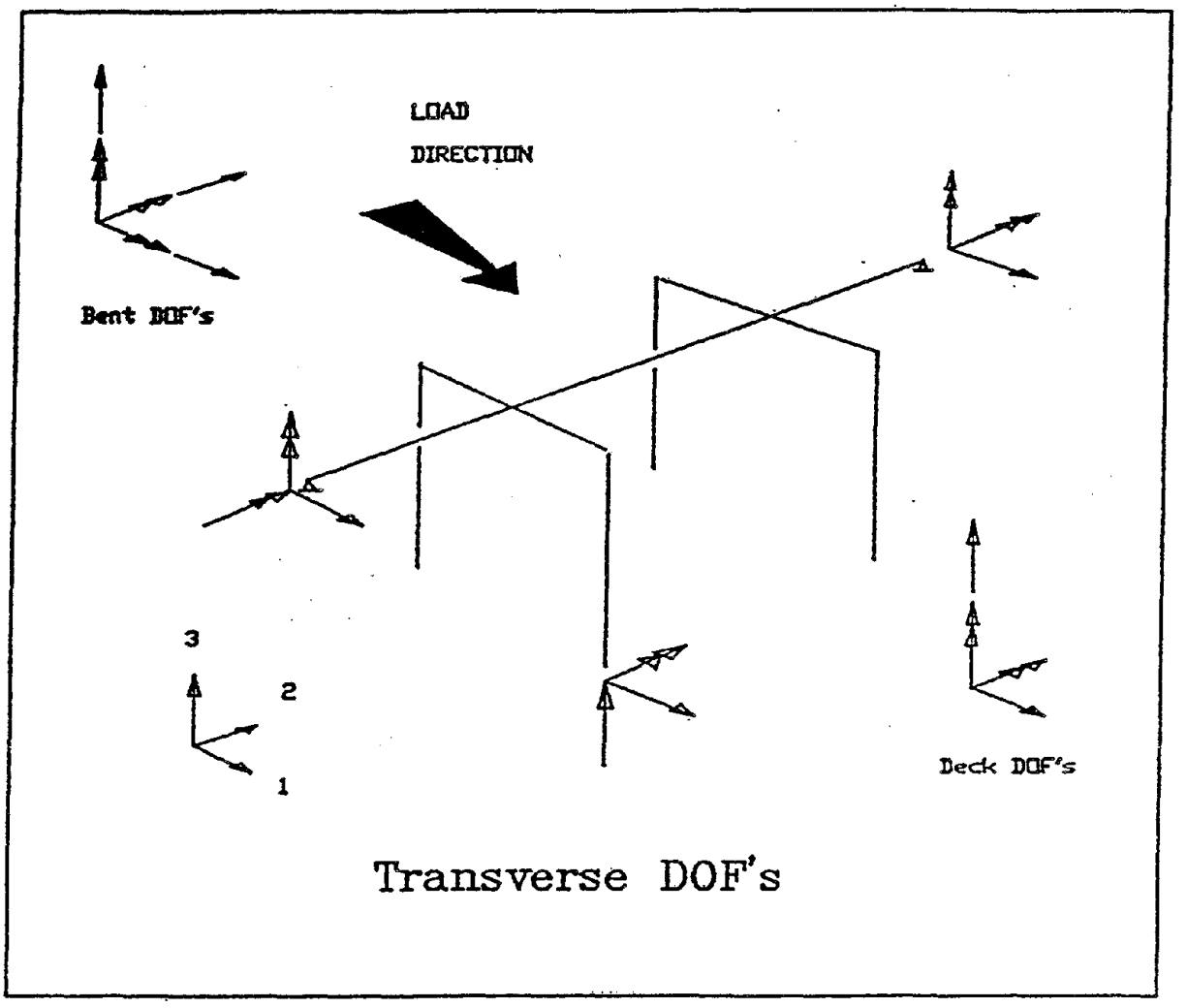

Figure 2.5 - Transverse Loading - Degrees of Freedom

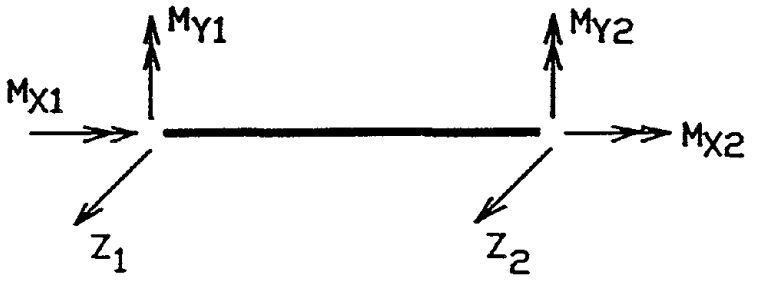

Figure 2.6 - Unrestrained DOF's for Transverse Deck Element

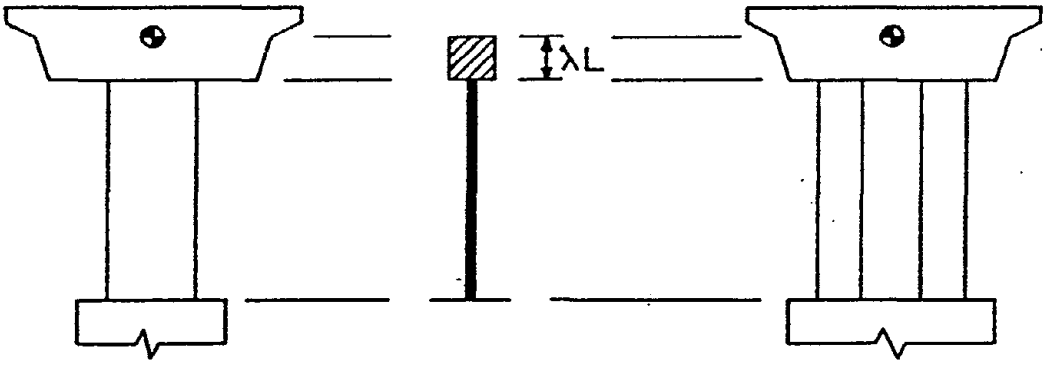

Figure 2.7 - Column Element Idealization

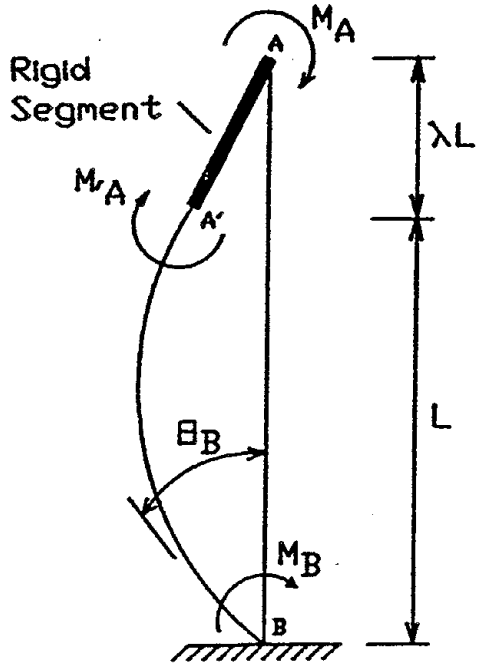

Figure 2.8 - Deformed Shape of Column Element (No Lateral Displacement)

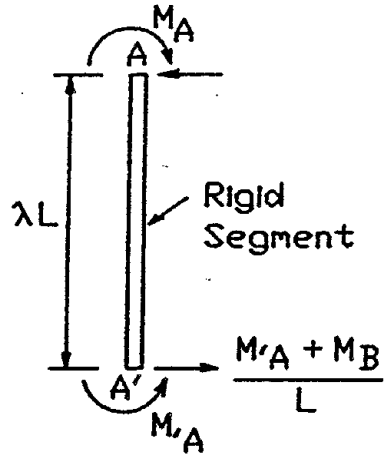

Figure 2.9 - Transformation of Moment for Column Rigid Segment

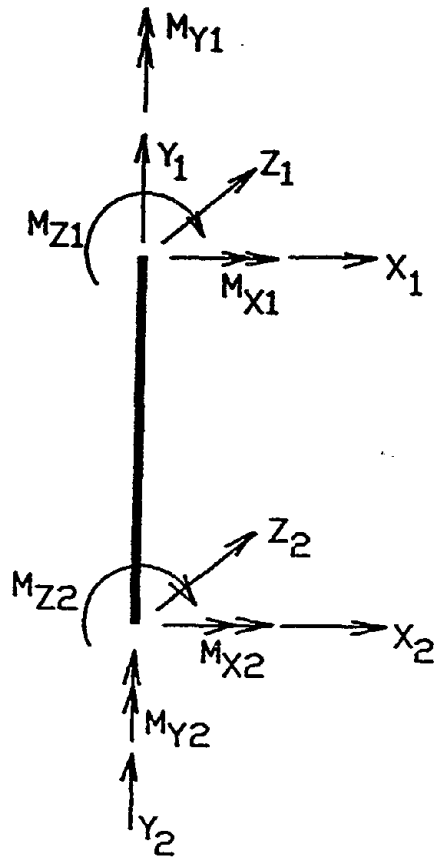

Figure 2.10 - Unrestrained Column Element DOF's for Transverse Model (Y1 = Y2)

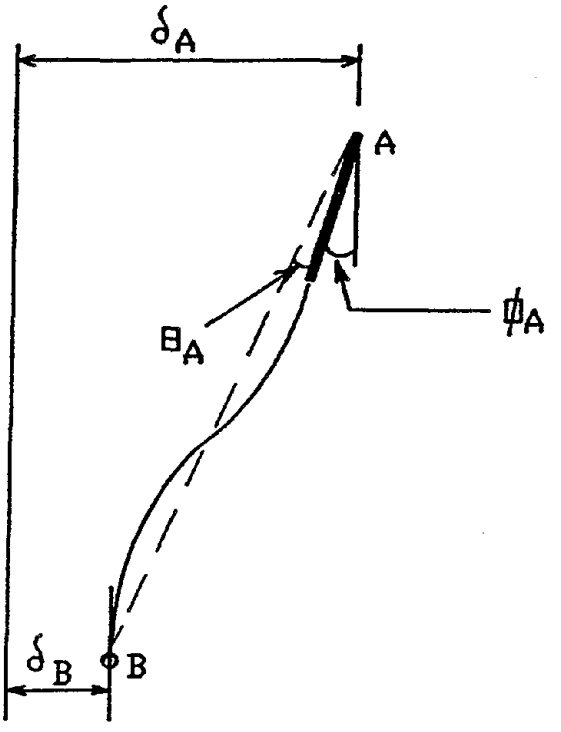

Figure 2.11 - Column Displacement-Rotation Relationship

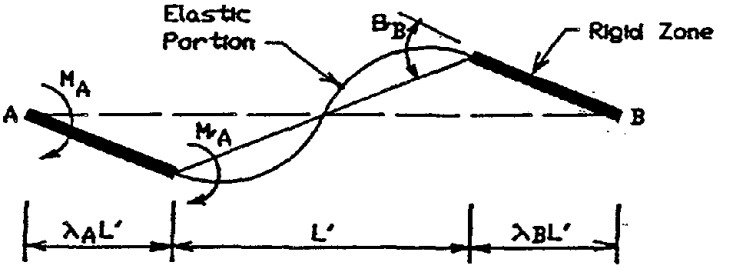

Figure 2.12 - Deformed Shape of Bent Cap Element (Transverse Loading) and Deck Element (Longitudinal Loading)

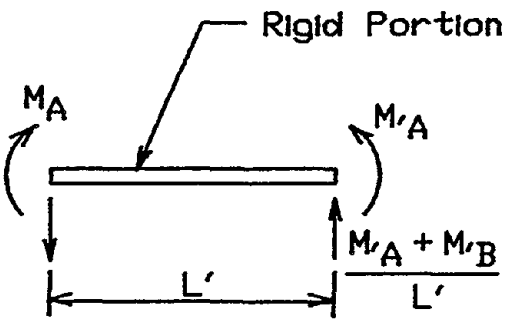

Figure 2.13 - Equillibrium of Rigid-End Segment

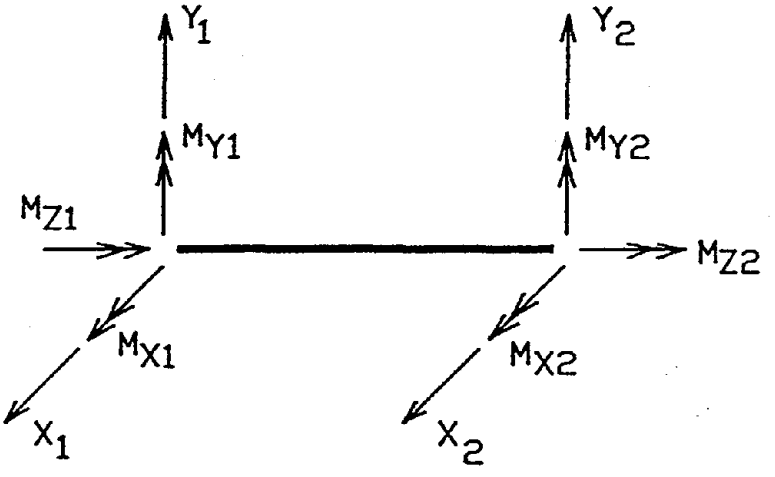

Figure 2.14 - Unrestrained Transverse Bent Cap DOF's

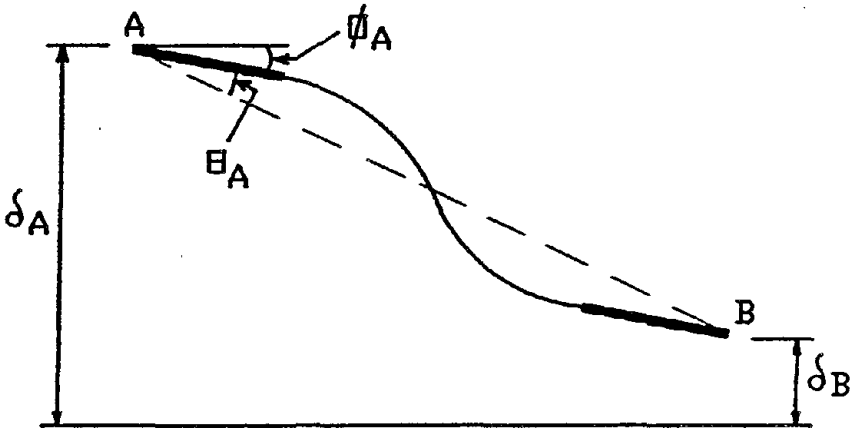

Figure 2.15 - Bent Cap (Transverse Model) and Deck (Longitudinal Model) Displacement-Rotation Relationship

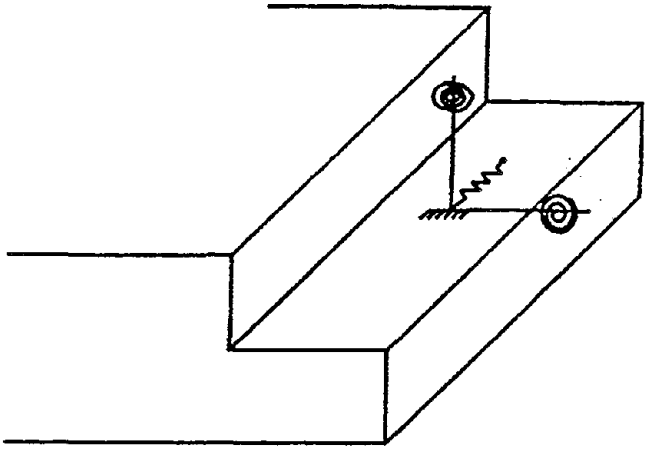

Figure 2.16 - Expansion Joint Spring Idealization

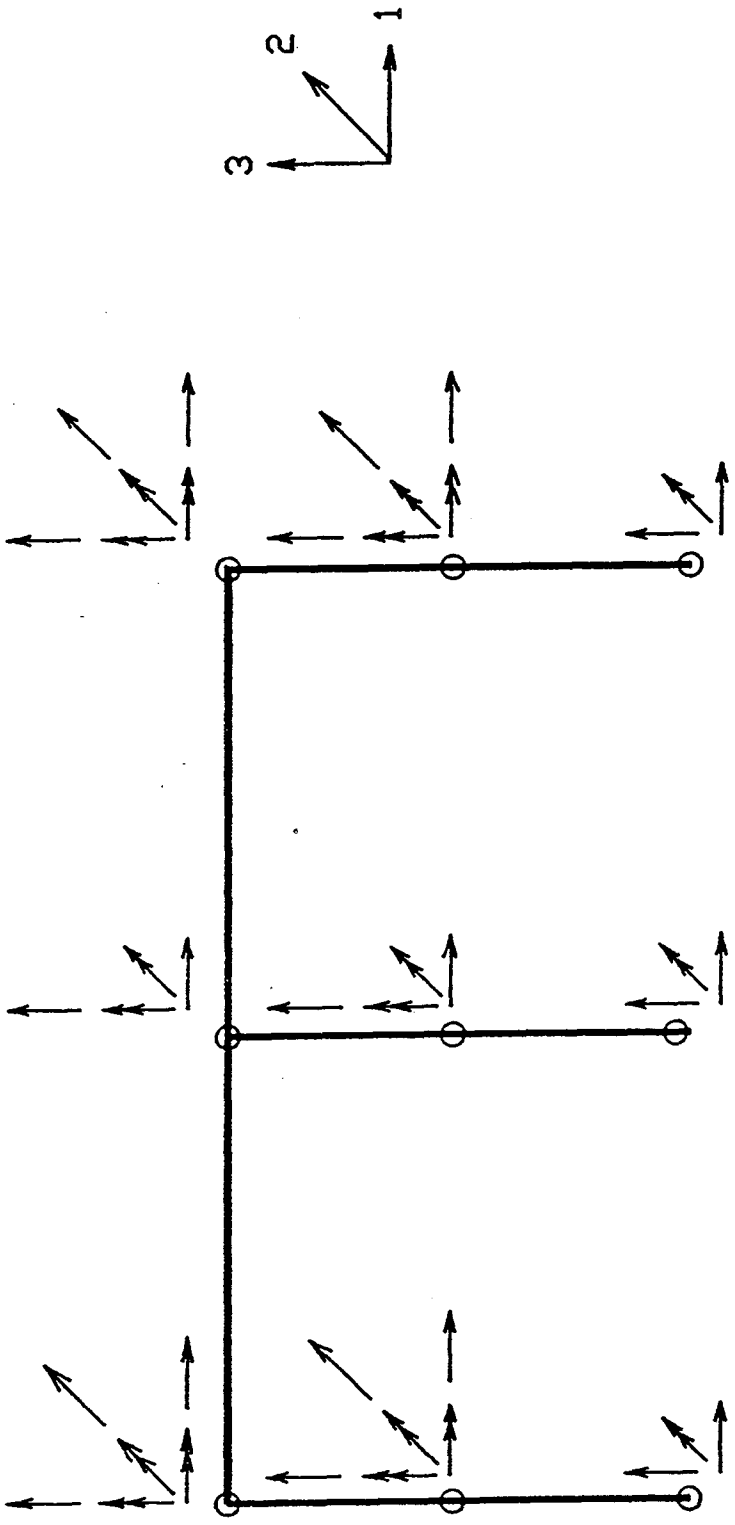

Figure 2.17 - Unrestrained Transverse Bent DOF's

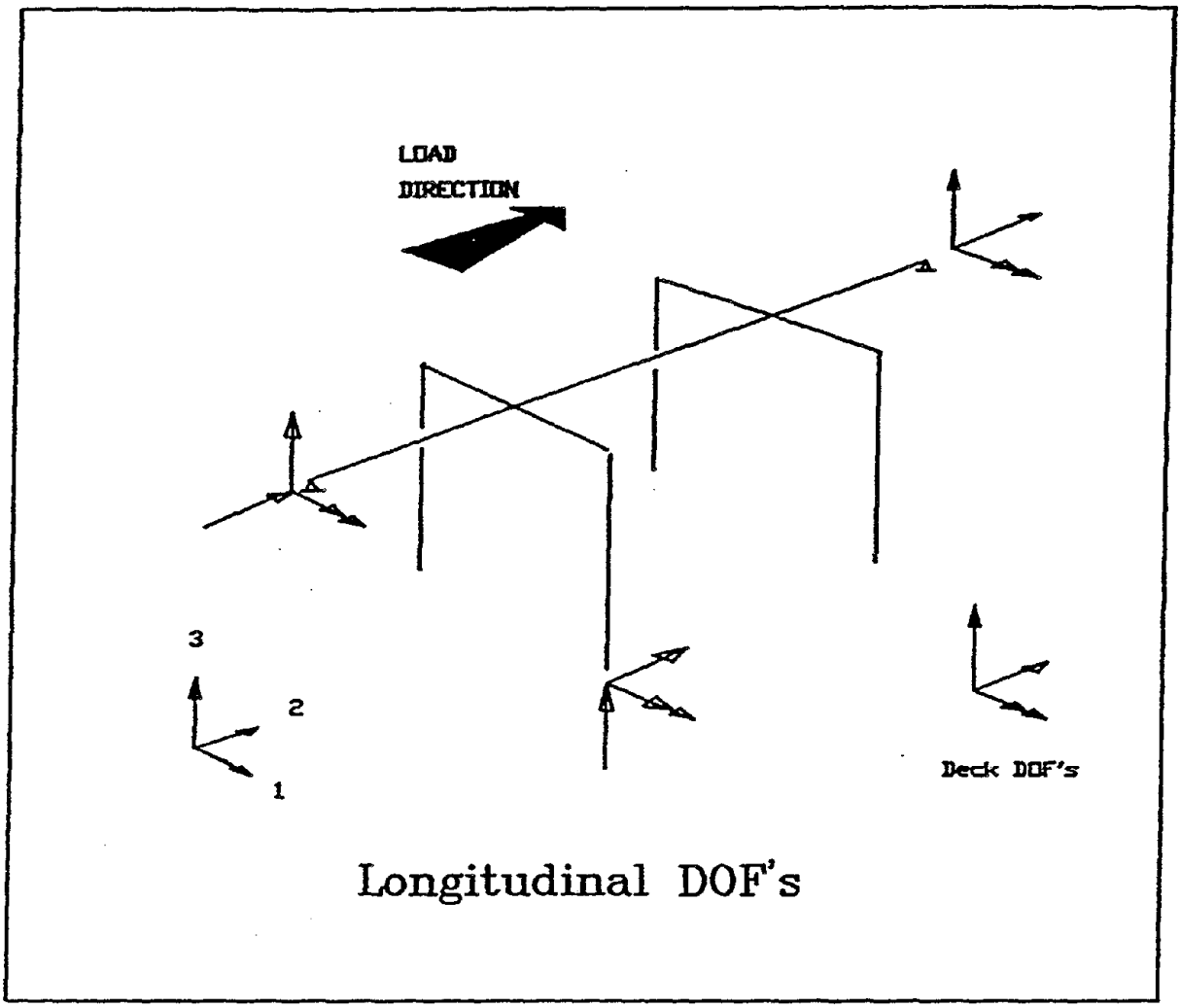

Figure 2.18 - Longitudinal Loading - Degrees of Freedom

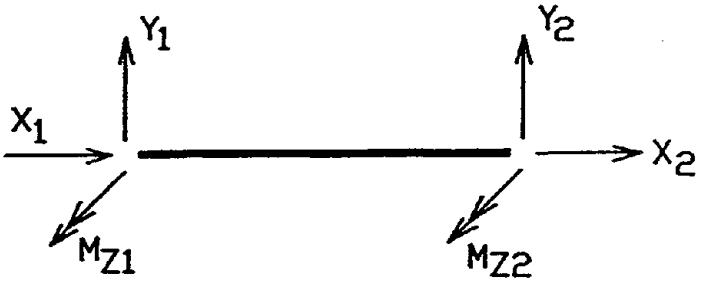

Figure 2.19 - Unrestrained Longitudinal Deck DOF's

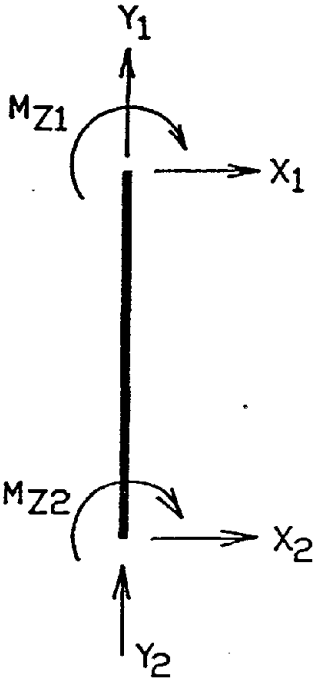

Figure 2.20 - Unrestrained Longitudinal Column Element DOF's (Y1 = Y2)

Figure 2.21 - Unrestrained Longitudinal Bent Cap DOF's

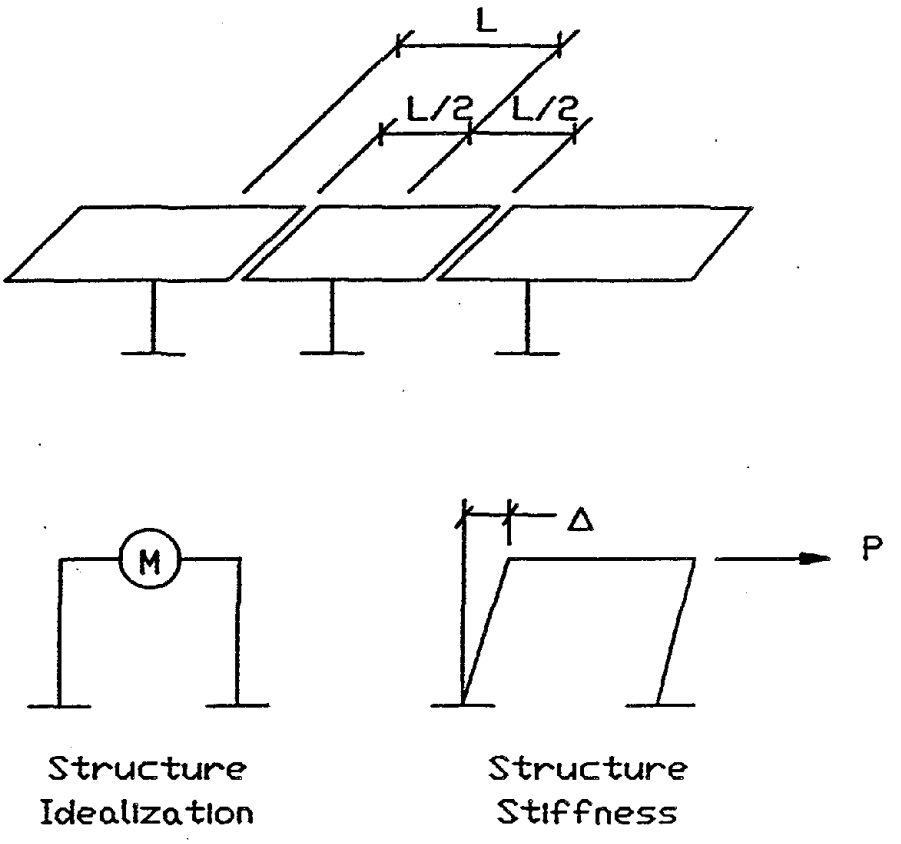

Figure 3.1 - The "Lollipop" Method

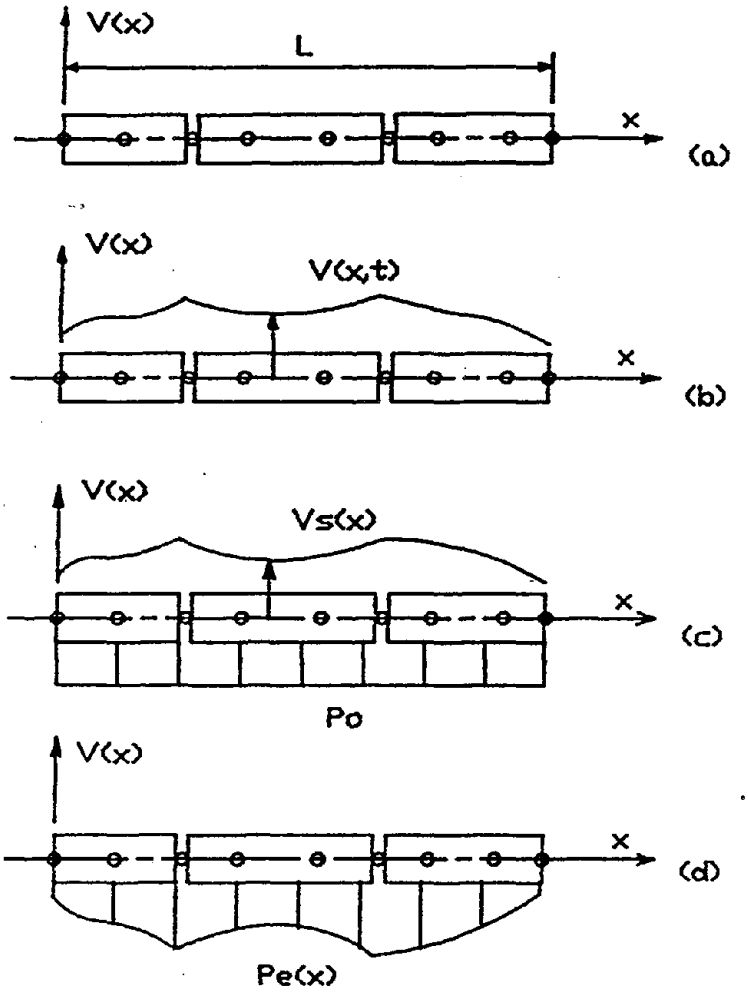

Figure 3.2 - a) Typical Bridge Configuration
b) Displacement Function
c) Fundamental Mode Shape Due to Uniform Unit Load
d) Psuedo Inertial Loading

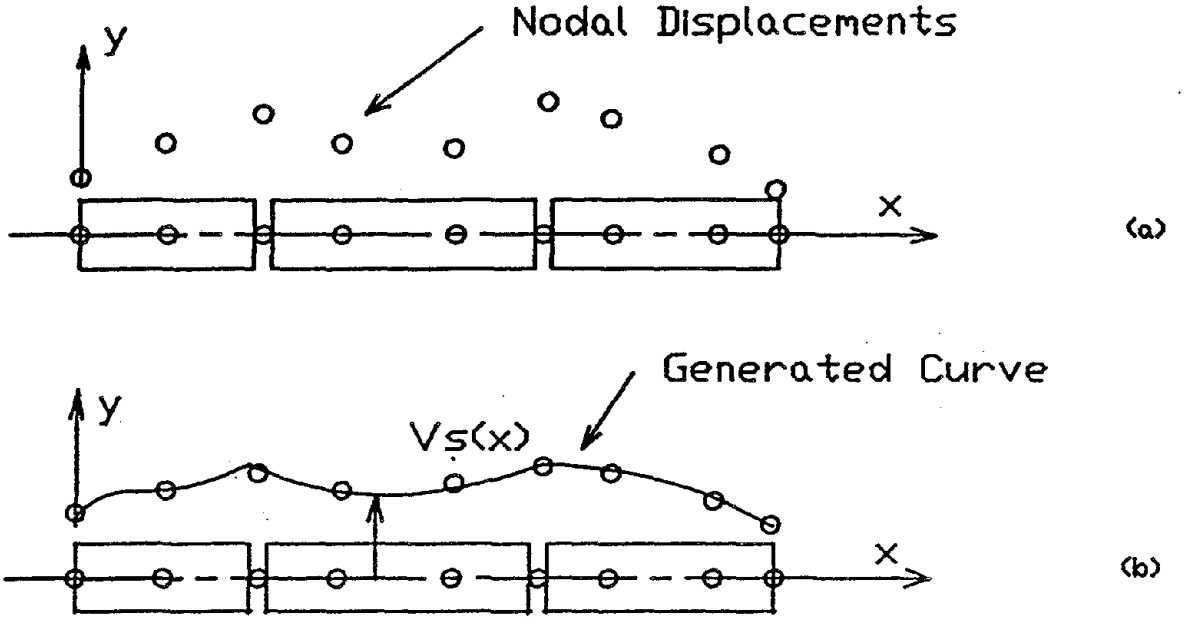

Figure 3.3 - Curve Fitting

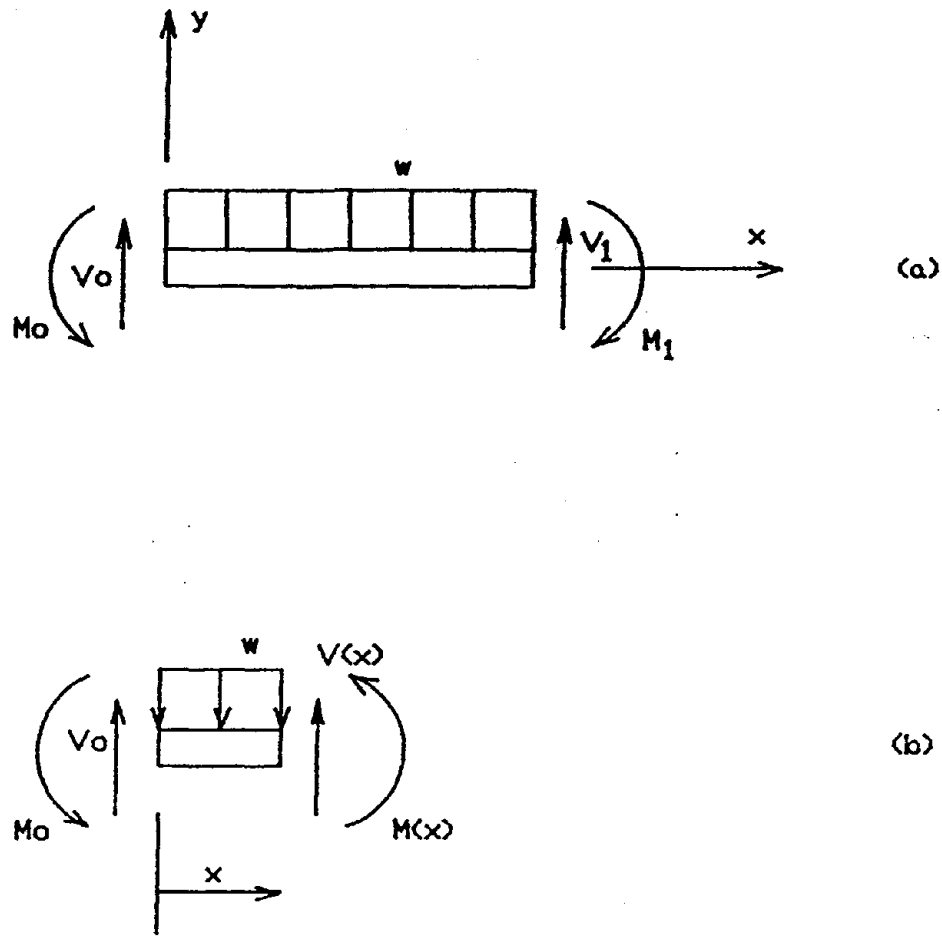

Figure 3.4 - Forces on a Deck Element

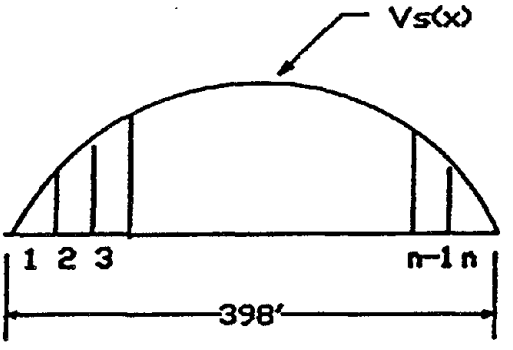

$$\alpha = \int Vs(x)dx$$

Direct Integration

$$Vs(x) = -0.085398 + 0.060857x - 0.0001529x^2$$

$$\alpha = 1572.64$$

Simpson's Method (n=40)

$$\alpha = 1571.53$$

% Error = 0.071%

Figure 3.5 - Numerical Integration with Simpson's Rule

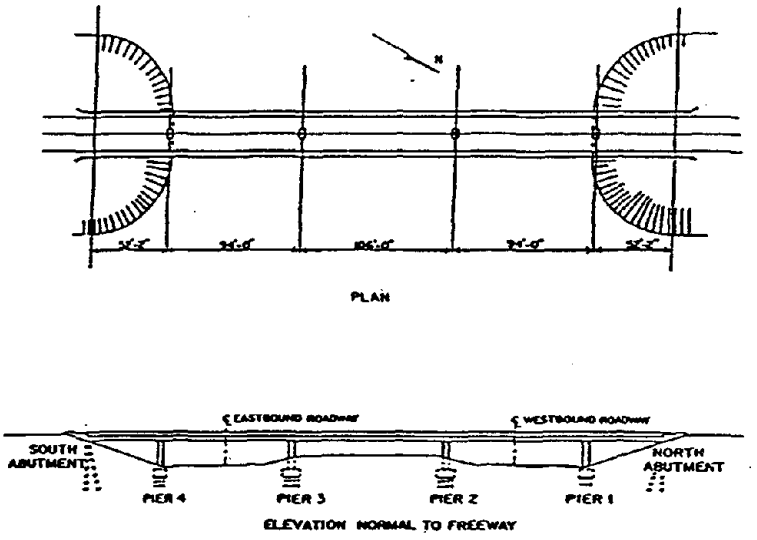

Figure 4.1 - Plan View and Elevation of the Rose Creek Bridge

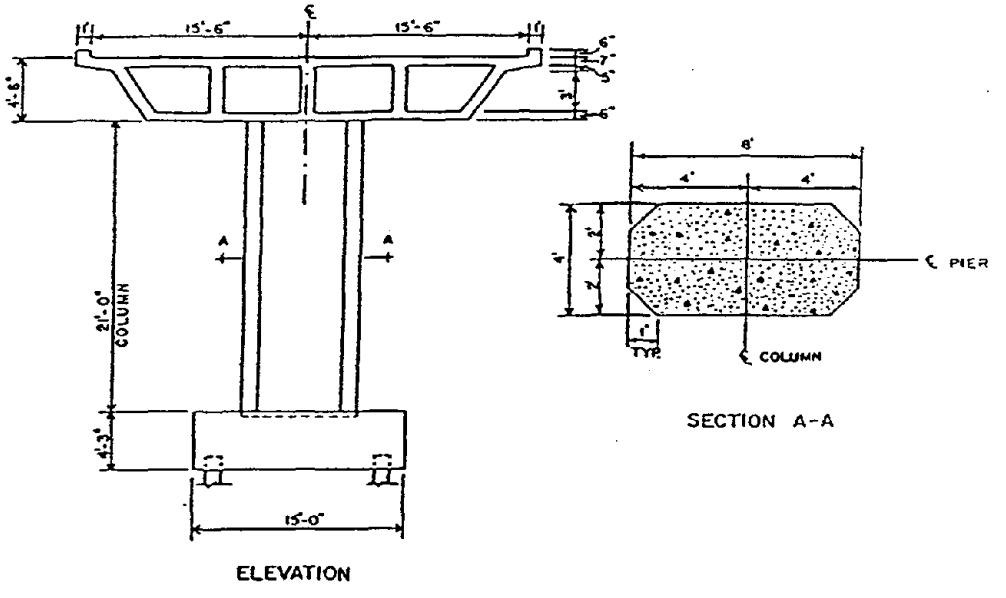

Figure 4.2 - Super- and Substructure Detail

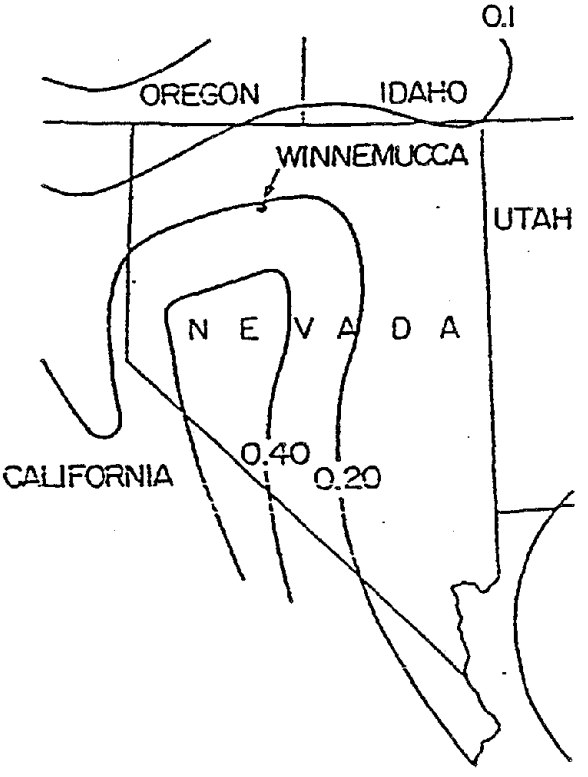

Figure 4.3 - Acceleration Coefficient Isocurves for Nevada

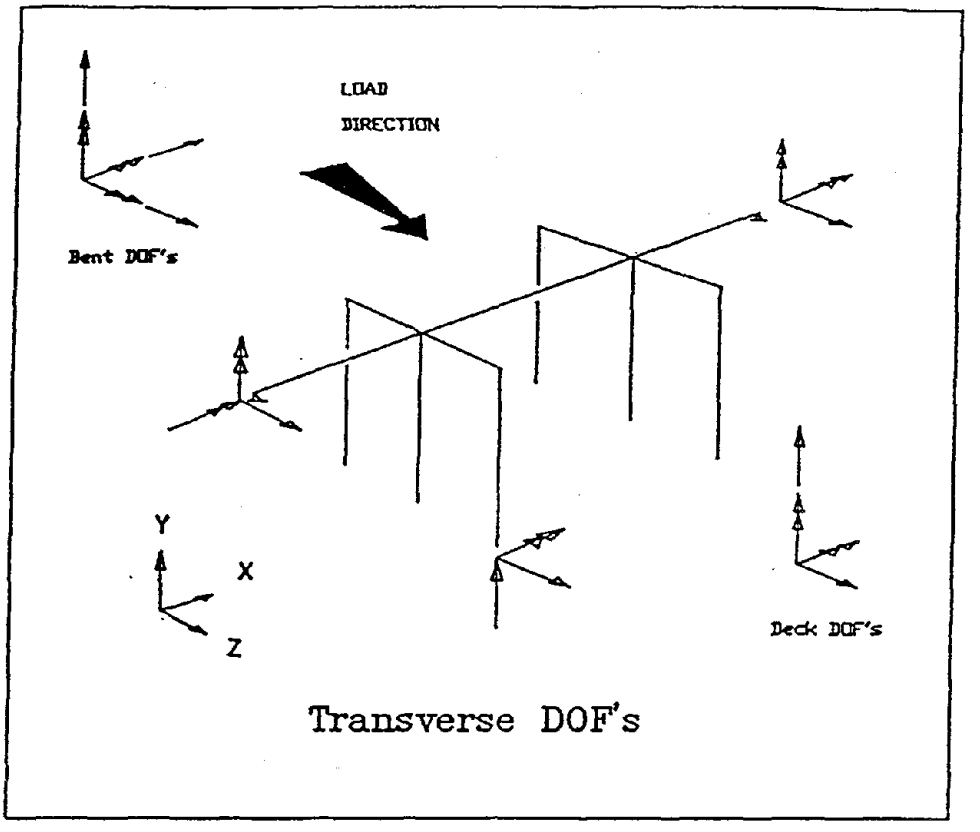

Figure 4.4 - Transverse Loading - Degrees of Freedom

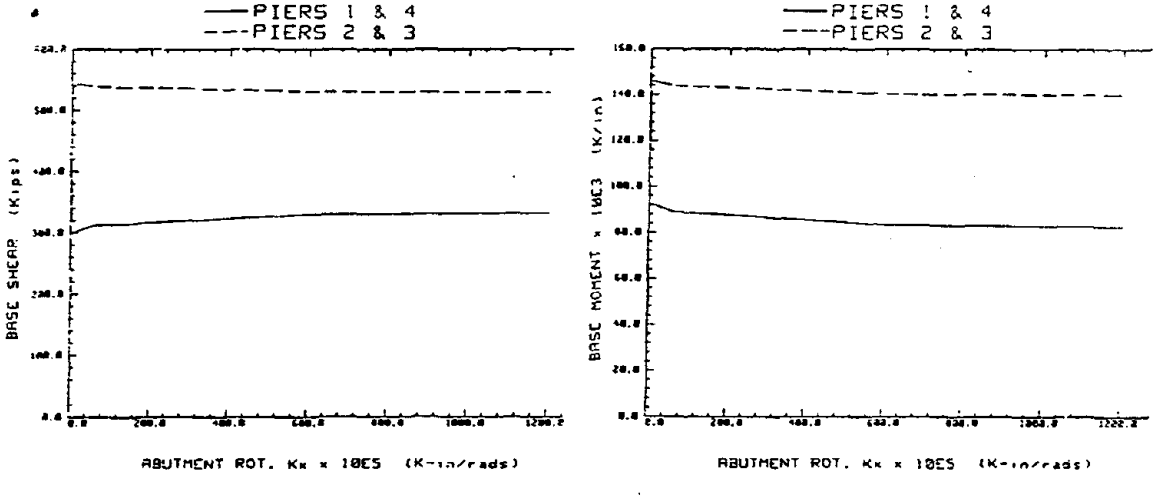

Figure 4.5 - Effect of Abutment Rotational Stiffness About the X Axis

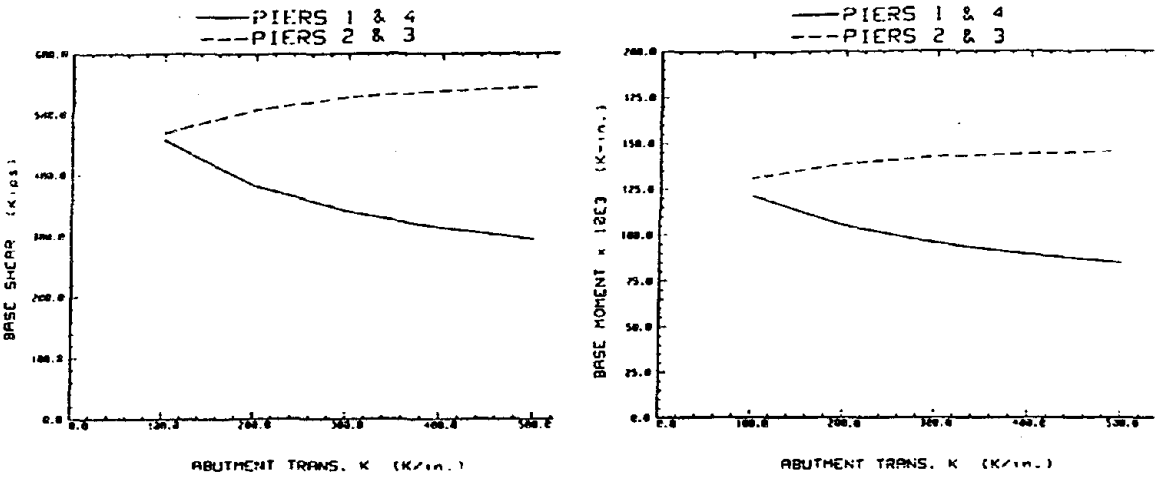

Figure 4.6 - Effect of Abutment Shear Stiffness

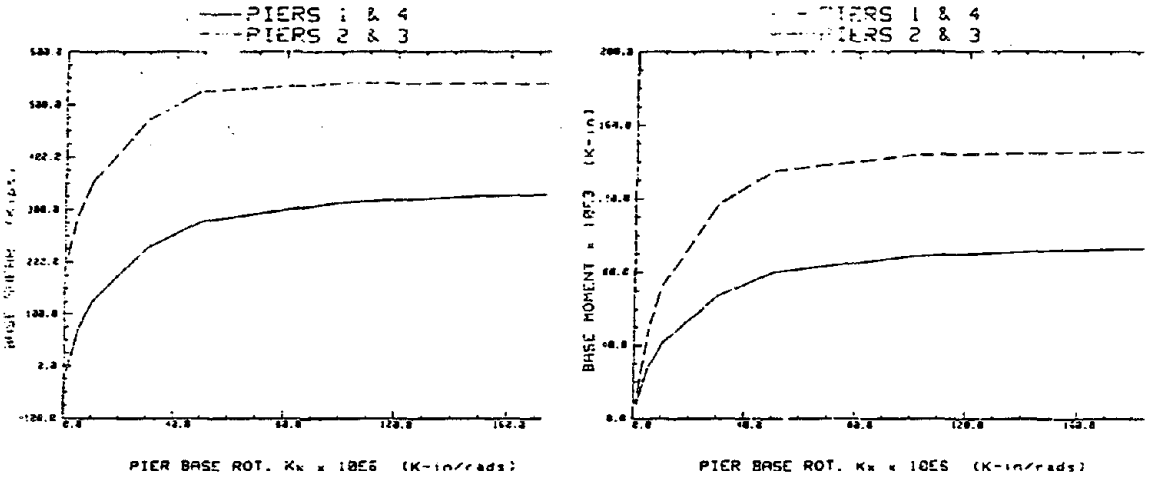

Figure 4.7 - Effect of Pier Foundation Rotational Stiffness About the X axis

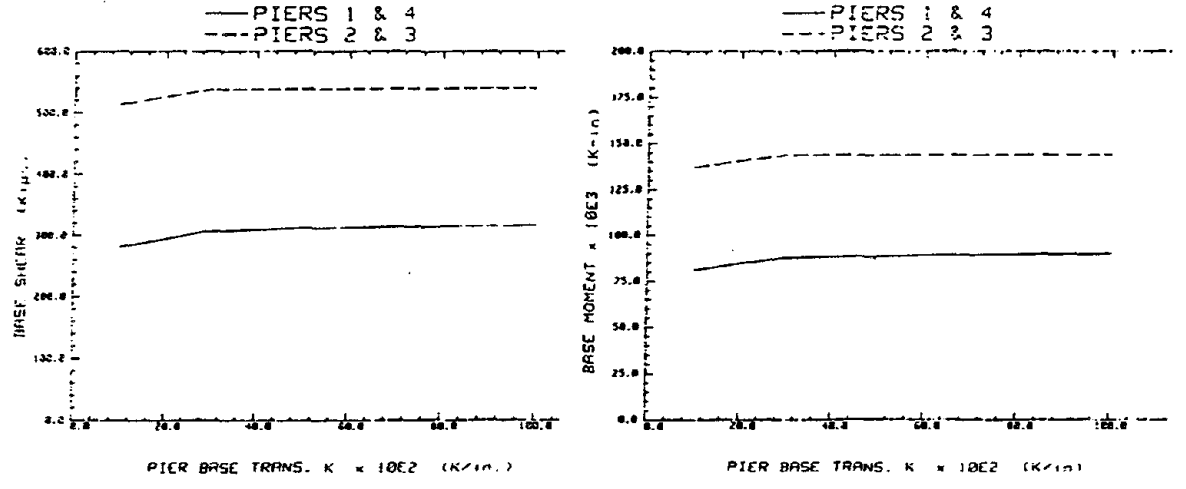

Figure 4.8 - Effect of Pier Foundation Translational Stiffness in Z Direction

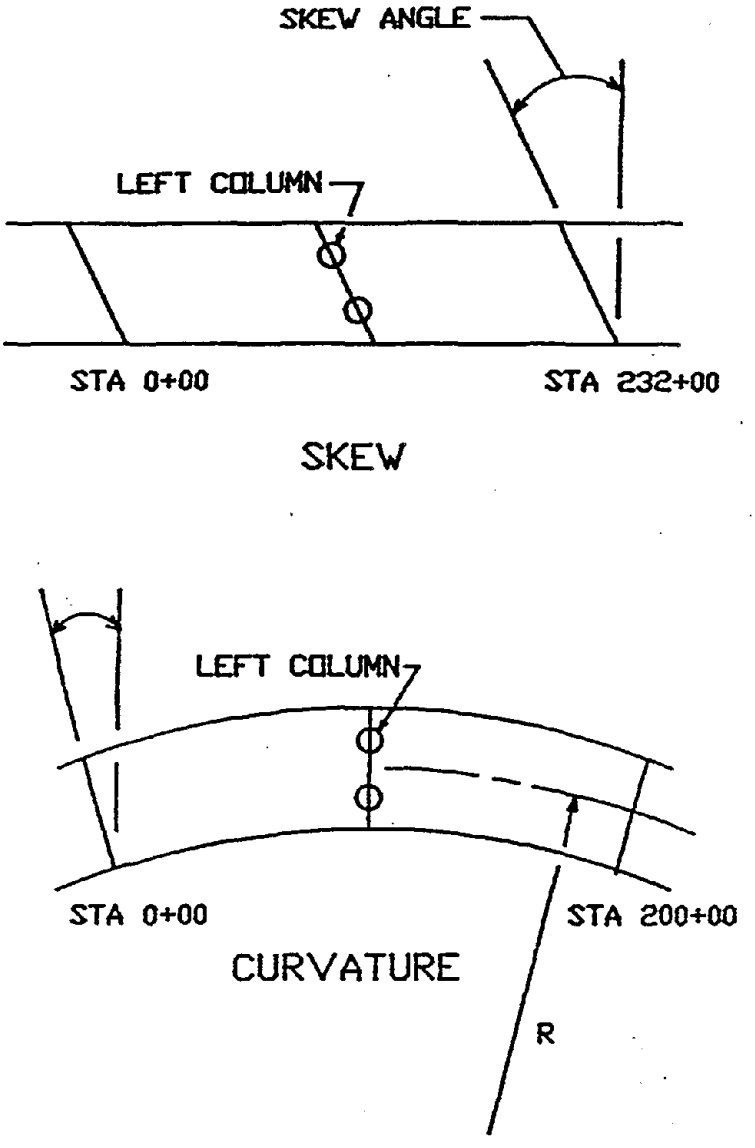

Figure 4.9 - Effects of Skew and Curvature

ROUTE 113/80 SEPERATION (WEST)

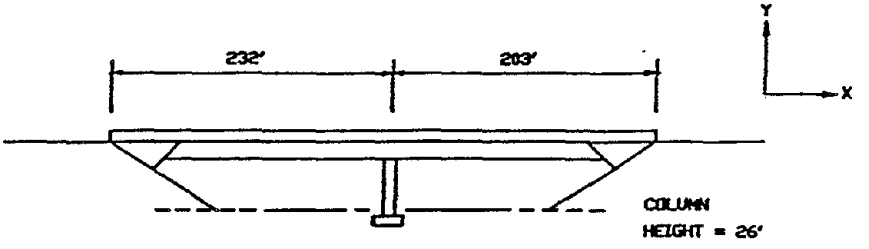

ELEVATION

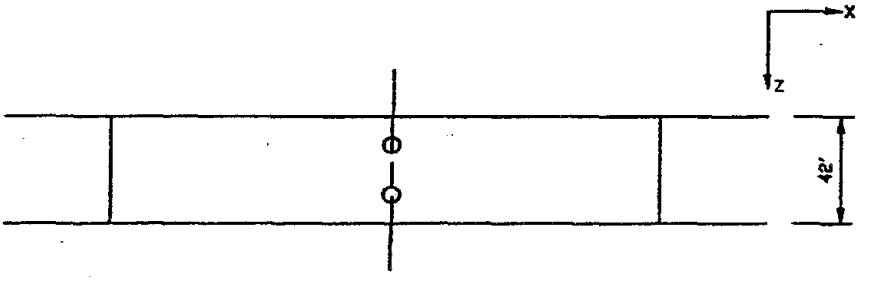

PLAN

STRUCTURAL DATA

SUPERSTRUCTURE:

A = 80 Ft.^{2}

Ix = 1791 Ft.^{4}

Iy = 11092 Ft.^{4}

Iz = 718.6 Ft.^{4}

E = 3850 ksi (554400 ksf)

COLUMN (Circ.):

Dia. = 5 Ft.

A = 19.63 Ft.^{2}

Ix = Iz = 30.68 Ft.^{4}

Iy = 61.35 Ft.^{4}

E = 4360 ksi (622840 ksf)

Note: SPECIAL BENT CAP Iz = 77 Ft.^{4}

Figure 4.10 - The Example Bridge for the Sensitivity Study

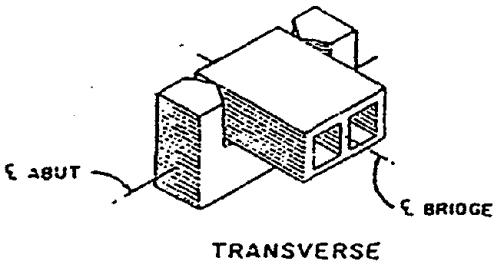

Figure 4.11 - Abutment Hinge Connectivity

APPENDIX A

MICROSARB TESTS EXAMPLES

Introduction

The example problems included in this publication illustrate the capabilities of the Microcomputer-Based Seismic Analysis of Regular Bridges (MicroSARB) computer program which can be used to implement Procedure 1 of the ATC-6 Seismic Design Guidelines.

These examples demonstrate the accurary of the model by comparing the results obtained from MicroSARB with those obtained using the mainframe program Seismic Analysis of Bridges (SEISAB). In addition dissimilarities between the MicroSARB and SEISAB models will be examined.

The following format is used in presenting each example problem:

- The objective of each example is discussed
- A brief description of the bridge being analyzed is presented
- Important modeling details are given
- Tables comparing MicroSARB and SEISAB results for a) deck displacements due to a unit load b) ATC-6 procedure 1 coefficients and c) deck displacements due to a psuedo seismic load are provided
- The output as pertaining to the comparison between MicroSARB and SEISAB is discussed

In some examples both transverse and longitudinal directions are presented, whereas, in others only transverse results are given.

In all cases the axial and shear deformations are neglected.

EXAMPLE 1

ANALYSIS OF A SINGLE-SPAN BRIDGE

Objective

This example illustrates the use of MicorSARB in analyzing a single-span reinforced concrete box-girder bridge. This example demonstrates the accuracy of modeling the deck elements.

Description of the Bridge

This bridge is a hypothetical example using real bridge properties. The box-girder spans are prismatic and are comprised of normal weight concrete. Abutments are assumed to be rigid and are restrained from displacement and rotation in all directions except the longitudinal direction. The longitudinal displacement is assumed to be free.

Modeling Details

The bridge has an overall span length 120.5 feet. The section properties of the bridge are displayed in figure A.1.1. A uniform unit weight of 20.3 kips/ft. is used to represent the weight of the concrete and all other components along the length of the bridge.

All of the abutment springs except the longitudinal displacement spring are assigned values of 1.0E10. The longitudinal displacement spring is assigned a value of 1.0E-10.

An Acceleration Coefficient (A) of 0.4 and a Site Coefficient (S) of 1.2 for Soil Profile Type II are assumed for this bridge site.

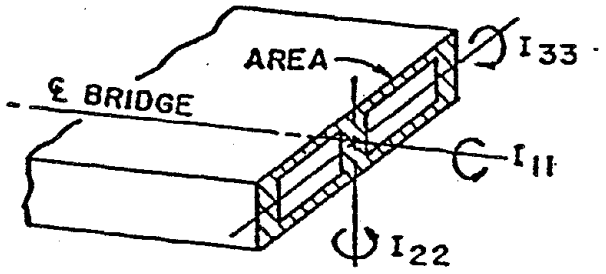

SUPERSTRUCTURE PROPERTIES

$A = 123\ ft^2$
$I_{1-1} = 117\ ft^4$
$I_{2-2} = 65550\ ft^4$
$I_{3-3} = 527\ ft^4$
$f'c = 3250\ psi$

Figure A.1.1 - Example 1 - Bridge Deck Properties

Comparison MicroSARB vs. SEISAB

Single Span Bridge:

Transverse Displacement Due to a Unit Load

Node #	MicroSARB	SEISAB	% Error
1	1.205E-08	1.205E-08	0.00
2	1.592E-05	1.592E-05	0.00
3	2.607E-05	2.607E-05	0.00
4	1.592E-05	1.592E-05	0.00
5	1.205E-08	1.205E-08	0.00

Alpha, Beta, Gamma, and T - Period

Parm.	MicroSARB	SEISAB	% Error
Alpha	0.0017828	0.0018253	2.33
Beta	0.0361923	0.0370551	2.33
Gamma	7.215E-07	7.399E-07	2.49
T-period	0.0223	0.0222928	0.03

Transverse Displacements Due to a Pseudo Seismic Load

Item	MicroSARB	SEISAB	% Error
Abut 1	1.816E-07	1.856E-07	2.21
Node 2	3.167E-04	3.196E-04	0.90
Node 3	5.327E-04	5.369E-04	0.79
Node 4	3.167E-04	3.196E-04	0.90
Abut 5	1.816E-07	1.856E-07	2.21

Comparison MicroSARB vs. SEISAB

Single Span Bridge:

Longitudinal Displacements Due to a Unit Load

Node #	MicroSARB	SEISAB	% Error
1	6.025E-02	6.025E-02	0.00
2	6.025E-02	6.025E-02	0.00
3	6.025E-02	6.025E-02	0.00
4	6.025E-02	6.025E-02	0.00
5	6.025E-02	6.025E-02	0.00

Alpha, Beta, Gamma, and T - Period

Parm.	MicroSARB	SEISAB	% Error
Alpha	7.26012	7.26013	.00
Beta	147.381	147.381	0.00
Gamma	8.879680	8.879680	0.00
T-period	1.2246	1.2246	0.00

Longitudinal Displacements Due to a Psuedo Seismic Load

Item	MicroSARB	SEISAB	% Error
Abut 1	0.615490	0.615490	0.00
Node 2	0.615490	0.615490	0.00
Node 3	0.615490	0.615490	0.00
Node 4	0.615490	0.615490	0.00
Abut 5	0.615490	0.615490	0.00

Discussion of the Comparison

A comparison between MicroSARB and SEISAB indicates that for both the transverse and the longitudinal directions the displacements due to a unit load are exact. Also in the longitudinal direction the ATC-6 parameters and the displacements due to a psuedo seismic load compare exactly.

In the transverse direction the ATC-6 parameters and the displacements due to a psuedo seismic load do not agree exactly between the two models. This apparent disagreement results because the generation of the curve which represents the displaced shape in the transverse direction is different for the two models.

In the MicroSARB model the displaced shape for each deck element is generated by using the flexural beam equation for a uniformly loaded beam with known end shears and moments, as well as, the known initial conditions; displacement and rotation. This results in a fourth-order equation to represent the flexural deformation of the bridge. The MicroSARB model uses Simpson's Rule to numerically integrate the displaced shape when generating the ATC-6 parameters and the psuedo seismic nodal loads.

In the SEISAB model the known nodal displacements and rotations are used in conjunction with the method of cubic splines to generate a series third-order equations (splines) to represent the deformed shape of the bridge. This model considers a closed-form solution for calculating the ATC-6 parameters and the psuedo seismic nodal loads.

EXAMPLE 2

ANALYSIS OF A FIVE-SPAN BRIDGE

Objective

This example illistrates the use of MicorSARB in analyzing a five-span reinforced concrete box-girder bridge with single column piers. This example demonstrates the effects of modeling bent elements (columns) and abutment and pier base spring elements.

Description of the Bridge

The bridge used in this example is the Rosecreek interchange located in Winnemuca, Nevada. The box-girder spans are prismatic and comprised of normal weight concrete. Seat-type abutments and pile footings at the pier bases provide longitudinal and transverse stiffness. All four piers consist of 21 foot long columns with 6 inch hinges at the foundation to column interface. The deck to pier connection is monolithic.

Modeling Details

A plan and elevation of the bridge is provided in figure A.2.1. The section properties and a cross-sectional view of the deck spans and columns are displayed in figure A.2.2. A uniform unit weight of 0.8083 kips/in. is specified and accounts for the weight of the concrete and all other components along the length of the bridge.

Abutment spring stiffness are specified as follows:

(transverse)	transverse displacement spring = 4.0E2 longitudinal rotational spring = 6.0E6 vertical rotational spring = 3.0E5
(longitudinal)	longitudinal displacment spring = 1.0E-10 vertical displacement spring = 5.0E9 transverse rotational spring = 5.0E9

Pier base spring stiffness are specified as follows:

(transverse)	transverse displacement spring = 5.0E3 longitudinal rotational spring = 1.0E8 vertical displacement spring = 5.0E9
(longitudinal)	longitudinal displacement spring = 5.0E9 vertical displacement spring = 5.0E9 transverse rotational spring = 5.0E9

An Acceleration Coefficient of 0.21 and a Site Coefficient of 1.2 for a Soil Profile Type II are used.

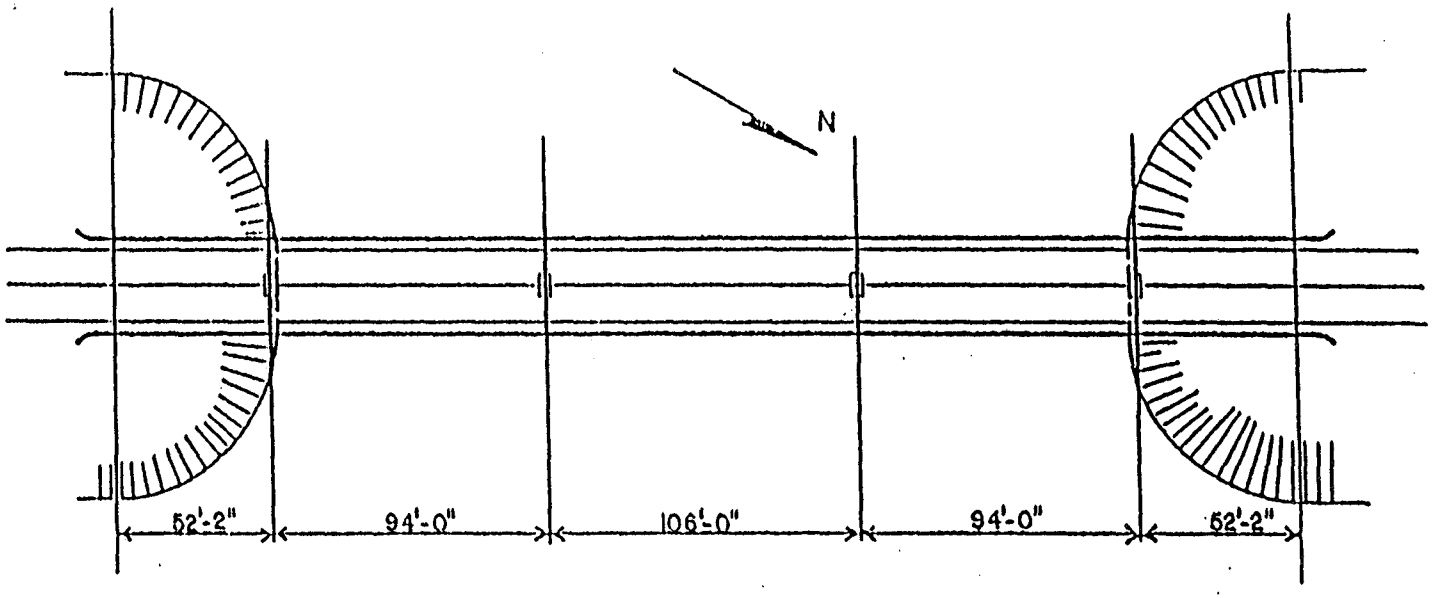

PLAN

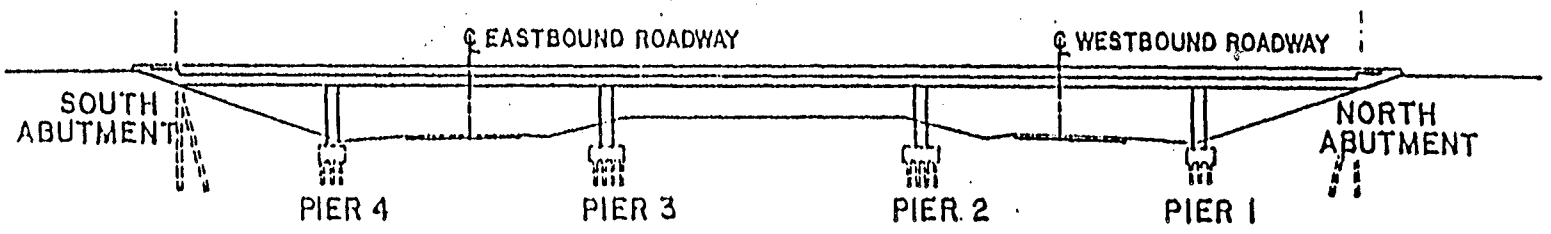

ELEVATION NORMAL TO FREEWAY

Figure A.2.1 - Planview and Elevation of Rose Creek Bridge

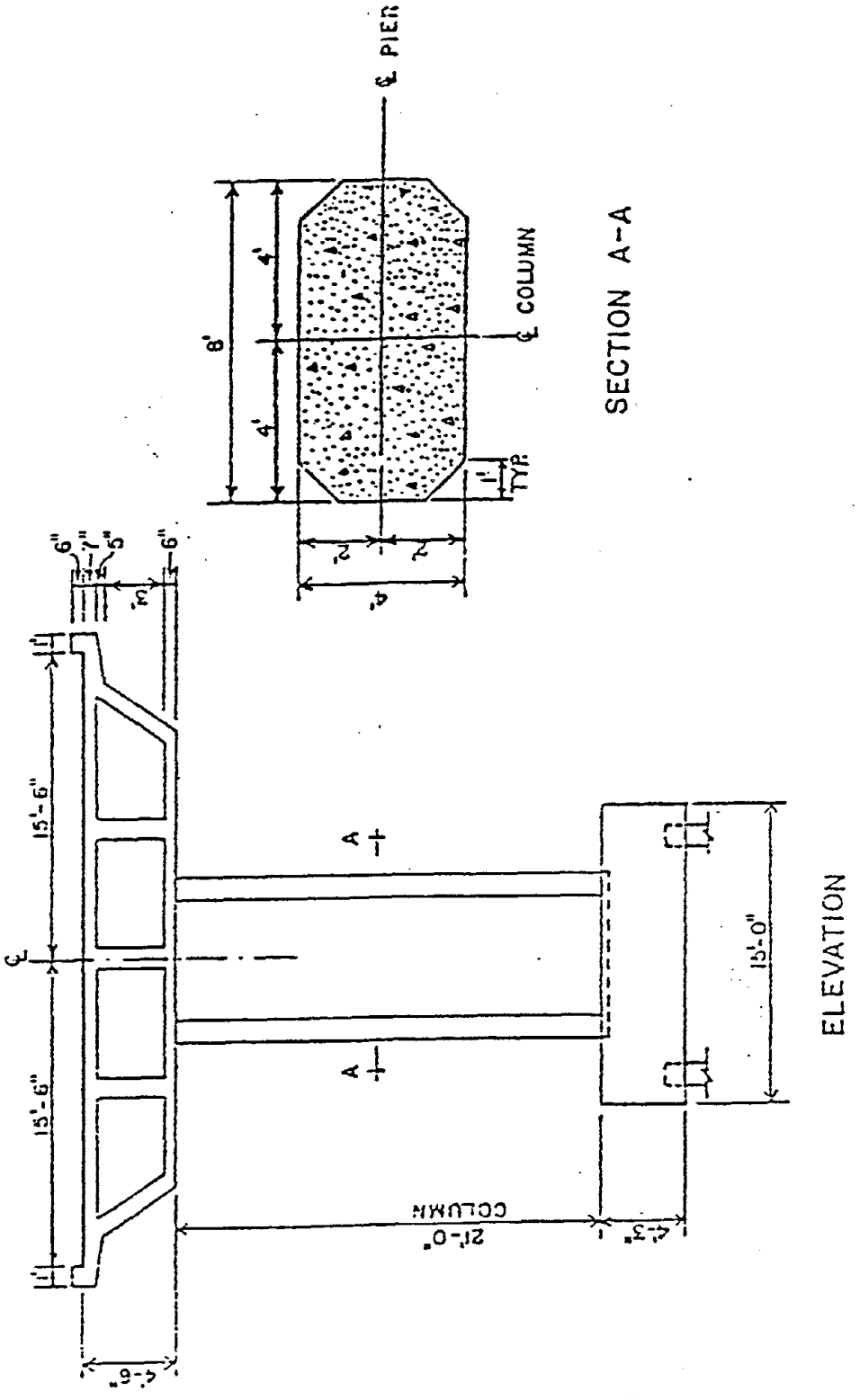

Figure A.2.2 - Pier Elevation

Comparison MicroSARB vs. SEISAB

Rosecreek Bridge: 5 span bridge with single column piers

Transverse Displacement Due to a Unit Load

Node #	MicroSARB	SEISAB	% Error
1	0.828149	0.828543	0.0476
2	0.984035	0.984337	0.0307
3	1.13483	1.13503	0.0176
4	1.27847	1.27857	0.0078
5	1.41623	1.41622	0.0007
6	1.65124	1.65015	0.0660
7	1.8397	1.83941	0.0158
8	1.96895	1.96859	0.0183
9	2.06158	2.06117	0.0199
10	2.15969	2.15922	0.0218
11	2.2019	2.20141	0.0223
12	2.15969	2.15922	0.0218
13	2.06158	2.06117	0.0199
14	1.96895	1.96859	0.0183
15	1.8397	1.83941	0.0158
16	1.65124	1.65105	0.0115
17	1.41623	1.41622	0.0007
18	1.27847	1.27857	0.0078
19	1.13483	1.13503	0.0176
20	0.984035	0.984336	0.0306
21	0.828149	0.828543	0.0476

Alpha, Beta, Gamma, and T - Period

Parm.	MicroSARB	SEISAB	% Error
Alpha	8217.52	8216.375	0.0139
Beta	6642.22	6641.296	0.0139
Gamma	12068.7	12065.01	0.0306
T-period	0.3874	0.387	0.1033

Transverse Displacements Due to a Psuedo Seismic Load

Item	MicroSARB	SEISAB	% Error
Abut 1	0.20593	0.2153	4.3521
Bent 2	0.53964	0.5397	0.0111
Bent 3	0.94801	0.9413	0.7078
Bent 4	0.94801	0.9413	0.7078
Bent 5	0.53964	0.5397	0.0111
Abut 6	0.20593	0.2153	4.3521

Comparison MicorSARB vs. SEISAB

Rosecreek Bridge: 5 span bridge with single column piers

Longitudinal Displacements Due to a Unit Load

Node #	MicroSARB	SEISAB	% Error
1	2.244	2.24373	0.0120
2	2.244	2.24373	0.0120
3	2.244	2.24373	0.0120
4	2.244	2.24373	0.0120
5	2.244	2.24373	0.0120
6	2.244	2.24373	0.0120
7	2.244	2.24373	0.0120
8	2.244	2.24373	0.0120
9	2.244	2.24373	0.0120
10	2.244	2.24373	0.0120
11	2.244	2.24373	0.0120
12	2.244	2.24373	0.0120
13	2.244	2.24373	0.0120
14	2.244	2.24373	0.0120
15	2.244	2.24373	0.0120
16	2.244	2.24373	0.0120
17	2.244	2.24373	0.0120
18	2.244	2.24373	0.0120
19	2.244	2.24373	0.0120
20	2.244	2.24373	0.0120
21	2.244	2.24373	0.0120

Alpha, Beta, Gamma, and T - Period

Parm.	MicroSARB	SEISAB	% Error
Alpha	10726.5	10725	0.0140
Beta	8670.25	8669.03	0.0141
Gamma	19456.4	19450.9	0.0283
T-period	0.4305	0.43046	0.0093

Longitudinal Displacements Due to a Psuedo Seismic Load

Item	ATC6PRC1	SEISAB	% Error
Abut 1	0.95228	0.9521	0.0189
Bent 2	0.95228	0.9521	0.0189
Bent 3	0.95228	0.9521	0.0189
Bent 4	0.95228	0.9521	0.0189
Bent 5	0.95228	0.9521	0.0189
Abut 6	0.95228	0.9521	0.0189

Discussion of the Comparison

In both the transverse and longitudinal directions the results obtained for displacements due to a uniform unit load as well as the ATC-6 parameters seem to compare quite well.

The displacements due to a seismic load are very accurate for the longitudinal direction. However, the results for the transverse direction indicate some discrepency in the generation of the seismic load. There is significant error at the abutments.

The MicroSARB model uses a direct equation of the elastic curve for each deck element to generate the displaced configuration fo the bridge. In the SEISAB model the method of cubic splines is used to generate the displaced shape.

EXAMPLE 3

ANALYSIS OF A THREE-SPAN BRIDGE

Objective

This example illustrates the use of MicroSARB in performing an analysis of a three-span bridge as described in the ATC-6 Seismic Design Guidlines for Highway Bridges. This example demonstrates the accuracy of MicroSARB for analyzing bridges with multicolumn bents.

Description of Bridge

The box girder spans are prismatic and composed of normal weight concrete. Seat-type abutments are used, and the abutment-to-superstructure connections are restrained only in the transverse direction. The bents are oriented normal to the bridge centerline. The bents are comprised of three identical 25 foot long reinforced concrete columns, spaced 35 feet on-center and centered on the bridge centerline. The connection between the bent caps and the superstructure is monolithic.

Modeling Details

The section properties of the bridge and the bridge layout are listed in Figure A.3.1. The weight of the concrete, the side railing, and other miscellaneous items are accounted for by applying a uniform unit load equal to 20.3 kips/ft. along the length of the bridge.

For loading in the transverse direction the transverse displacement spring and the longitudinal rotational spring are assigned a value of 1.0E10, and the vertical rotational spring is assigned a value of 1.0E-10 in-order-to model the abutment-to-superstructure connection as a hinge. All pier base springs are given values of 1.0E10 to model a rigid pier base.

In the longitudinal direction all abutment and pier base springs except for the abutment longitudinal displacement spring are assigned values of 1.0E10. The abutment longitudinal displacement spring equals 1.0E-10.

A Soil Profile Type II (S = 1.2) and Acceleration Coefficient of 0.4 are assumed for this bridge site.

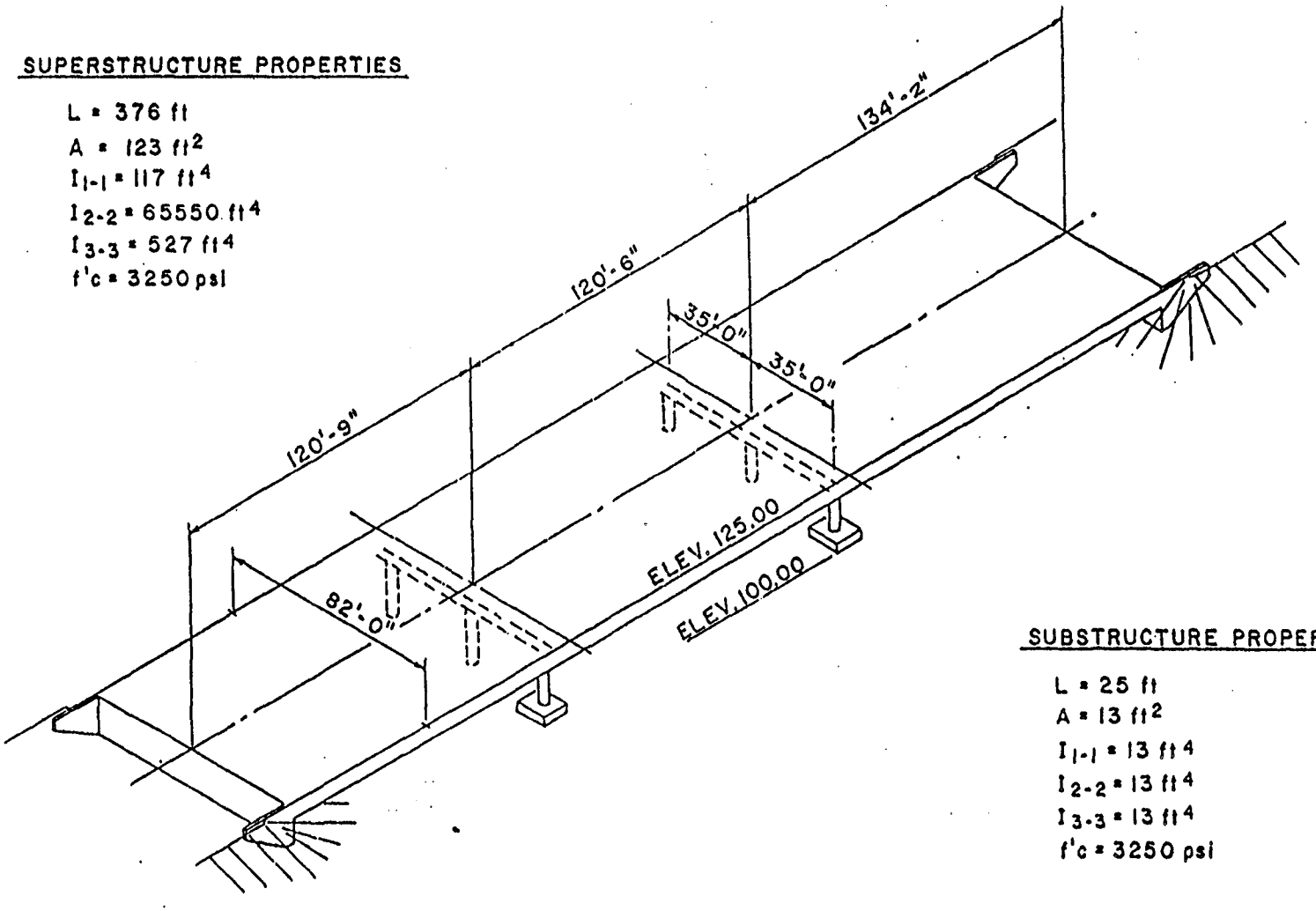

Figure A.3.1 - Elevation of Three-Span Bridge and Super- and Substructure Properties

Comparison MicroSARB vs. SEISAB

ATC6 Example Bridge: 3 span bridge with 3 column bents

Transverse Displacement Due to a Unit Load

Node #	MicroSARB	SEISAB	% Error
1	2.626E-08	2.623E-08	0.0823
2	0.0013935	0.0013946	0.0846
3	0.0026765	0.0026790	0.0918
4	0.0037656	0.0037696	0.1048
5	0.0046065	0.0046123	0.1247
6	0.0051669	0.0051742	0.1409
7	0.0054124	0.0054201	0.1437
8	0.0053245	0.0053319	0.1399
9	0.0049143	0.0049204	0.1250
10	0.0041091	0.0041134	0.1050
11	0.0029691	0.0029719	0.0932
12	0.0015618	0.0015631	0.0857
13	2.683E-08	2.681E-08	0.0835

Alpha, Beta, Gamma, and T - Period

Parm.	MicorSARB	SEISAB	% Error
Alpha	1.3101	1.312	0.1450
Beta	26.5951	26.626	0.1162
Gamma	0.113654	0.114	0.3044
T-period	0.3261	0.327	0.2760

Transverse Displacements Due to a Psuedo Seismic Load

Item	MicroSARB	SEISAB	% Error
Abut 1	3.910E-07	3.898E-07	0.3000
Bent 2	0.0936005	0.09368	0.0849
Bent 3	0.100121	0.1002	0.0788
Abut 4	4.036E-07	4.025E-07	0.2627

Comparison MicroSARB vs. SEISAB

ATC6 Example Bridge: 3 span bridge with 3 column bents

Longitudinal Displacements Due to a Unit Load

Node #	MicroSARB	SEISAB	% Error
1	0.016066	0.016066	0.0000
2	0.016066	0.016066	0.0000
3	0.016066	0.016066	0.0000
4	0.016066	0.016066	0.0000
5	0.016066	0.016066	0.0000
6	0.016066	0.016066	0.0000
7	0.016066	0.016066	0.0000
8	0.016066	0.016066	0.0000
9	0.016066	0.016066	0.0000
10	0.016066	0.016066	0.0000
11	0.016066	0.016066	0.0000
12	0.016066	0.016066	0.0000
13	0.016066	0.016066	0.0000

Alpha, Beta, Gamma, and T - Period

Parm.	MicroSARB	SEISAB	% Error
Alpha	6.04074	6.04097	0.0038
Beta	122.627	122.632	0.0041
Gamma	1.9701	1.97025	0.0076
T-period	0.6323	0.632353	0.0084

Longitudinal Displacements Due to a Psuedo Seismic Load

Item	MicroSARB	SEISAB	% Error
Abut 1	0.25499	0.25500	0.0039
Bent 2	0.25499	0.25500	0.0039
Bent 3	0.25499	0.25500	0.0039
Abut 4	0.25499	0.25500	0.0039

Discussion of the Comparison

For this bridge the results obtained for both the transverse and the longitudinal directions seem to compare very well between MicroSARB and SEISAB. More discrepency is apparent in the transverse direction when comparing the two models for the ATC-6 parameters and the transverse displacement due to a seismic load. This small error can be attributed to different approaches used to generate the curvature of the superstructure.

EXAMPLE 4

ANALYSIS OF A FIVE-SPAN BRIDGE

Objective

The ATC-6 Procedure 1 analysis in the transverse direction is performed on a five-span reinforced concrete bridge in this example. In this example the effectiveness of MicroSARB to analyze bridges with variable column heights is examined.

Description of the Bridge

A sketch of the continuos, reinforced concrete box-girder bridge is shown in Figure A.4.1. The abutment-to-superstructure connection is monolithic, and the abutments are assumed to be rigid. The bents are comprised of two circular prismatic columns and are oriented normal to the bridge centerline.

Modeling Details

The section properties of the superstructure and the substructure are displayed in Figure A.4.2. The circular reinforced concrete columns are spaced 31'-0" on center and are modeled as single prismatic segments. A bent cap is used and it has the following properties: flexural inertia about the longitudinal and vertical axes = 75.0, torsional inertia about the transverse axis = 1.0E10.

The fixed abutments are modeled by assuming all spring stiffness values of 5.0E9. The pier base spring stiffness values are: vertical and transverse displacement springs = 5.0E9, and the longitudinal rotational spring = 1.0E-10. This effectively models the column-to-foundation connection as pinned.

The Accelleration Coefficient is 0.21, and a Site Coefficient of 1.2 for a Soil Profile Type II is specified.

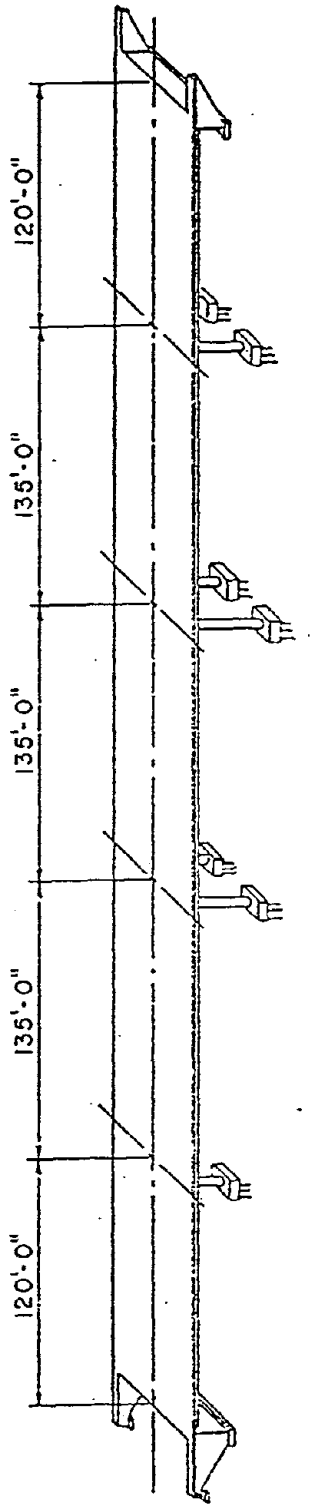

Figure A.4.1 - Elevation of Five-Span Bridge

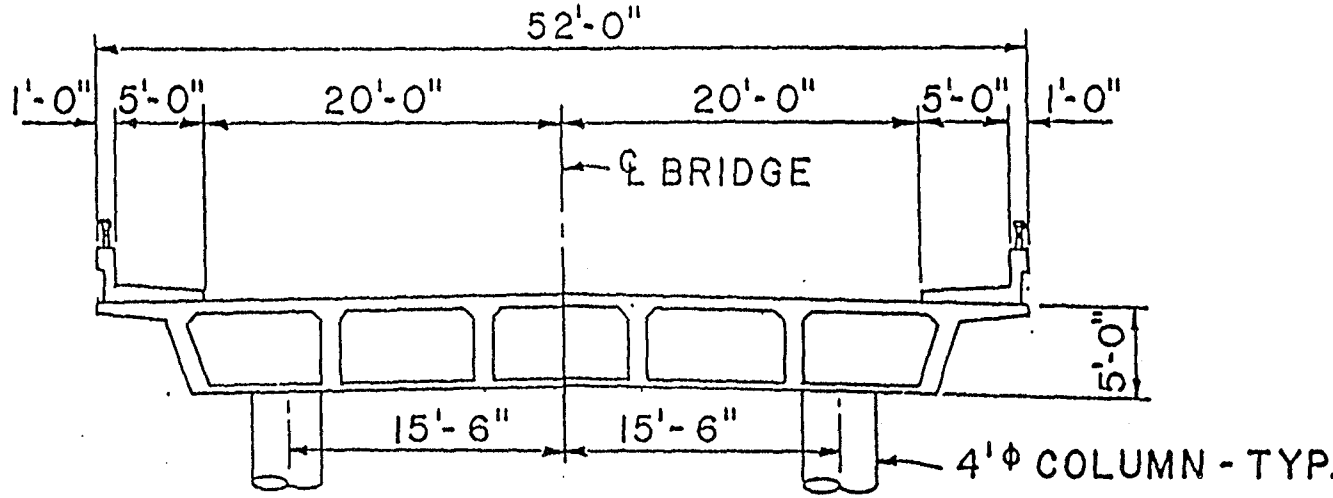

TYPICAL SECTION

SUPERSTRUCTURE

L = 750.0 ft

A = 105.0 ft^2

I_{1-1} = 900 ft^4

I_{2-2} = 17000.0 ft^4

I_{3-3} = 300 ft^4

SUBSTRUCTURE

A = 12.6 ft^2

I_{1-1} = 25.2 ft^4

I_{2-2} = 12.6 ft^2

I_{3-3} = 12.6 ft^2

Figure A.4.2 - Superstructure Cross-Section and Structural Properties

Comparison MicroSARB vs. SEISAB

Five Span Bridge: two column bents (three different types)

Transverse Displacements Due to a Unit Load

Node #	MicroSARB	SEISAB	% Error
1	6.9233E-09	6.9242E-09	0.01
2	6.6763E-02	6.6657E-02	0.16
3	1.7900E-01	1.7858E-01	0.24
4	1.9113E-01	1.9072E-01	0.21
5	9.3253E-02	9.3194E-02	0.06
6	8.5031E-09	8.5073E-09	0.05

Alpha, Beta, Gamma, and T - Period

Parm.	MicroSARB	SEISAB	% Error
Alpha	73.10013	72.186	1.25
Beta	1111.44	1099.028	1.12
Gamma	175.41	167.515	4.71
T-period	1.7164	1.687	1.71

Transverse Displacements Due to a Psuedo Seismic Load

Item	MicrSARB	SEISAB	% Error
Abut 1	-2.0286E-09	-1.4150E-09	43.36
Bent 2	1.4712E-01	1.4820E-01	0.73
Bent 3	6.1960E-01	6.3470E-01	2.38
Bent 4	6.8395E-01	7.0080E-01	2.40
Bent 5	2.4552E-01	2.5060E-01	2.03
Abut 6	3.5924E-09	5.0140E-09	28.35

Discussion of the Comparison

It is apparent in this example that the deformed superstructure generated by MicroSARB using equations of the elastic curve for each deck element is slightly different than the deformed shape created by SEISAB using cubic splines. Even though there is error between MicroSARB and SEISAB for final displacements, this error is very small and can be considered insignificant for this type of analysis. It is important to note that the displacements at the abutments are very small and thus the behavior of the abutments is very sensative to even very small changes in loading.

EXAMPLE 5

ANALYSIS OF A TWO-SPAN BRIDGE WITH AN INTERMEDIATE EXPANSION JOINT

Objective

In this example MicroSARB is used to analysis a two-span reinforced concrete box-girder bridge that includes an intermediate expansion joint in the left deck span. This example illustrates the effectiveness of modeling hinge elements.

Description of the Bridge

This bridge is a hypothetical example using real bridge properties. This bridge is comprised of elements from the Rosecreek Interchange bridge of Example 2. The spans and the pier are identical to the exterior spans and the piers used in Example 2. Seat-type abutments and a pile foundation at the pier base provide longitudinal and transverse stiffness.

Modeling Details

The bridge has an overall span length of 104 feet. The section properties of the spans and columns are displayed in Figure A.2.2. A uniform unit load of 0.8083 kips/in. accounts for the weight of the concrete and all other components along the length of the bridge.

For the transverse loading direction the abutment and pier base translational and rotational spring stiffnesses are the same as those shown in Example 2. For the expansion joint (loaded transversely) the spring stiffnesses are 1.0E10 for the transverse displacement and longitudinal rotational springs, and 1.0E-10 for the vertical rotational spring. This effectively models the expansion joint as a pinned hinge.

For the longitudinal loading direction all spring stiffnesses except the longitudinal translational spring are the same as those displayed in Example 2. The longitudinal displacement spring is assigned a value of 1000. For the expansion joint (loaded longitudinally) the spring stiffnesses are 1.0E10 for the transverse rotational spring and 1.0E-10 for the longitudinal and vertical displacement springs.

The Acceleration Coefficient and Site Coefficient are identical to those of Example 2.

Comparison MicroSARB vs. SEISAB

ROSEEXP : 2 span bridge, single column pier, expansion joint

Transverse Displacements Due to a Unit Load

Node #	MicroSARB	SEISAB	% Error
1	0.401999	0.401998	.00
2	1.10374	1.10363	0.01
3	1.80419	1.80396	0.01
4	1.80419	1.80396	0.01
5	1.56691	1.56672	0.01
6	1.33485	1.33469	0.01
7	1.11211	1.11199	0.01
8	0.893168	0.893078	0.01
9	0.673523	0.673467	0.01
10	0.452021	0.452	.00

Alpha, Beta, Gamma, and T - Period

Parm.	MicroSARB	SEISAB	% Error
Alpha	1395.1	1406.291	0.80
Beta	1127.66	1136.705	0.80
Gamma	1412.15	1448.028	2.48
T-period	0.3216	0.324	0.74

Transaverse Displacements Due to a Psuedo Seismic Load

Item	MicroSARB	SEISAB	% Error
Abut 1	0.122769	0.1192	2.91
Hinge 1	0.892133	0.8955	0.38
Bent 2	0.597928	0.597	0.16
Abut 3	0.0396245	0.03405	14.07

Comparison MicroSARB vs. SEISAB

ROSEEXP : 2 span bridge, single column pier, expansion joint

Longitudinal Deflection Due to a Unit Load

Node #	MicroSARB	SEISAB	% Error
1	0.313	0.313	0.00
2	0.313	0.313	0.00
3	0.313	0.313	0.00
4	0.61285	0.61284	.00
5	0.61285	0.61284	.00
6	0.61285	0.61284	.00
7	0.61285	0.61284	.00
8	0.61285	0.61284	.00
9	0.61285	0.61284	.00
10	0.61285	0.61284	.00

Alpha, Beta, Gamma, and T - Period

Parm.	MicroSARB	SEISAB	% Error
Alpha	673.436	650.323	3.55
Beta	544.338	525.656	3.55
Gamma	309.854	292.554	5.91
T-period	0.2168	0.2144	1.12

Longitudinal Displacements Due to a Psuedo Seismic Load

Item	MicroSARB	SEISAB	% Error
Abut 1	0.0730353	0.07307	0.05
Hinge 1	0.279997	0.2759	1.46
Bent 2	0.279997	0.2759	1.46
Abut 3	0.279997	0.2759	1.46

Discussion of the Comparison

Once again as in the previous examples the error between MicroSARB and SEISAB for displacements due to a unit load in the transverse and longitudinal direction is negligible. However, the error between the two models for the ATC-6 parameters and the displacements due to a psuedo seismic load becomes slightly more noticable.

As in previous examples the different methods used to generate the displaced shape of the superstructure in the transverse directions leads to small error for the ATC-6 parameters and final displacements.

In the longitudinal direction SEISAB uses cubic splines to generate a displaced configuration due to a unit load. Because axial deformations are being neglected the MicroSARB model assumes that the displacements along the length of each element are identical to the nodal displacements for the two nodes confining each particular element. In effect the MicroSARB model does not generate a curve representing the displaced configuration in the longitudinal direction.

EXAMPLE 6

ANALYSIS OF A THREE-SPAN BRIDGE

Objective

This example illustates the use of MicorSARB to analyze a three-span reinforced concrete bridge with two different bent types. The capability of MicroSARB to handle different bent types is demonstated by this example. Note: Only the transverse direction is examined.

Description of the Bridge

The bridge used in this example is identical to the one used in Example 3; however, the left bent is replaced with a single column pier identical to those of the Rosecreek Interchange (See Example 2).

Modeling Details

The section properties of the bridge superstructure are listed in Figure A.3.2. The bent section properties are listed in Figure A.2.2 (single column bent) and Figure A.3.2 (multicolumn bent). A uniform unit load of 20.3 kips/ft. accounts for the weight of the concrete and other miscell- aneous items. The abutment and pier base spring stiffnesses are identical to those discussed in Example 3. The Acceleration and Site Coefficients are identical to those of Example 3.

Comparison MicroSARB vs. SEISAB

MULTPIER : 3 Span bridge with 2 seperate pier types

Transverse Displacements Due to a Unit Load

Node #	MicroSARB	SEISAB	% Error
1	2.979E-08	2.978E-08	0.0400
2	0.0017715	0.0017717	0.0062
3	0.0034156	0.0034157	0.0029
4	0.0048312	0.0048315	0.0062
5	0.0059471	0.0059477	0.0096
6	0.0067124	0.0067132	0.0119
7	0.0070762	0.0070772	0.0138
8	0.0070054	0.0070064	0.0140
9	0.0064958	0.0064968	0.0143
10	0.0054354	0.0054363	0.0153
11	0.0039201	0.0039207	0.0135
12	0.0020574	0.0020577	0.0146
13	3.276E-08	3.276E-08	0.0104

Alpha, Beta, Gamma, and T - Period

Parm.	MicroSARB	SEISAB	% Error
Alpha	1.70987	1.71	0.0076
Beta	34.7104	34.714	0.0104
Gamma	0.19403	0.194	0.0155
T-period	0.373	0.373	0.0000

Transverse Displacements Due to a Pseudo Seismic Load

Item	MicroSARB	SEISAB	% Error
Abut 1	4.586E-07	4.578E-07	0.1849
Bent 2	0.120675	0.1206	0.0622
Bent 3	0.132303	0.1323	0.0023
Abut 4	5.263E-07	5.256E-07	0.1402

Discussion of the Comparison

The reults of the transverse loading seem to compare very well between the two models for all three categories. Once again a slightly larger difference is evident when comparing MicroSARB to SEISAB for the displacements due to a seismic load. It is obvious that the deformed shape generated using the equation of the elastic curve for the deck elements (MicroSARB) is very close to that generated using cubic splines (SEISAB).

APPENDIX B

MEMORY EFFICIENT PROGRAMMING

B.1 Introduciton

One disadvantage associatied with programming on microcomputers is the limited availability of memory space for storing large arrays of numbers. Because of these limitations the programmer must utilize memory-efficient programming techniques to reduce the amount of data stored in arrays.

B.2 List Processing

In the MicroSARB model, in an attempt to minimize memory requirements yet increase computational efficiency, an implicit list processing (ILP) technique was employed. For large matrices which can not be banded or triangularized it is more efficient to keep track of only the non-zero elements. The list processing technique is a means by which only the non-zero elements are stored in memory. In this type of list processing, once the values and locations of the non-zero elements are known the matrix can be manipulated. This can be referred to as an explicit list processing (ELP).

In ELP, two arrays are usually formed, one in which all the column numbers of the non-zero elements of the matrix are stored, and the other acting as a pointer to the first array, identifying the areas associated with each